Zoological Journal of the Linnean Society, 2026, **208**(3), zlag181
https://doi.org/10.1093/zoolinnean/zlag181
Original Article

OXFORD

A new bi-polar deep-sea genus of Isopoda *Bathyjaera* gen. nov. (Asellota: Janiridae), including the description of a new species from the Jøtul vent field in the Arctic Ocean

Katharina Kohlenbach[1,2,3,*], Emanuel Pereira[4,5], Saskia Brix[2,6], Katrin Linse[7]

[1]Deep-Sea Ecology and Technology, Alfred Wegener Institute, Helmholtz Center for Polar and Marine Research, Bremerhaven, 27570, Germany
[2]Benthic Biogeography, Institute of Marine Ecosystem and Fishery Science, University of Hamburg, Hamburg, 22767, Germany
[3]HGF MPG Joint Research Group for Deep-Sea Ecology and Technology, Max Planck Institute for Marine Microbiology, Bremen, 28359, Germany
[4]Departamento de Biodivesidad y Biología Experimental (DBBE), Facultad de Ciencias Exactas y Naturales, Universidad de Buenos Aires, Buenos Aires, 1428, Argentina
[5]Instituto de Biodiversidad y Biología Experimental y Aplicada (IBBEA), CONICET - Universidad de Buenos Aires, Buenos Aires, 1428, Argentina
[6]Senckenberg am Meer, German Centre for Marine Biodiversity Research (DZMB), Hamburg, 20146, Germany
[7]British Antarctic Survey, Cambridge, CB3 0ET, United Kingdom

[*]Corresponding author. Katharina Kohlenbach, Alfred-Wegener-Institut, Helmholtz-Zentrum für Polar-und Meeresforschung, Am Handelshafen 12, 27570 Bremerhaven, Germany. E-mail: katharina.kohlenbach@awi.de

Abstract

Bathyjaera **Kohlenbach and Linse gen. nov. is established for two species: the species *Bathyjaera tyleri* (Brandt and Malyutina, 2014) comb. nov. and *Bathyjaera giselae* Kohlenbach and Pereira sp. nov. The new genus is characterized by a broad body, absence of eyes, short antenna, peduncle article I shorter than articles II–IV, pereopods II–VII dactylus with small ventral claw, uropod exopod and endopod same length, wide pleotelson with a medial point in the caudal notch, short pleopods I with medial lobe triangular, and a bathyal distribution. *Bathyjaera giselae* Kohlenbach and Pereira sp. nov. was collected at the Nidhogg chimney (3016 m) in the Jøtul vent field and the deep-sea Amundsen Basin (4156 m) in the Arctic Ocean. The new species is designated as the type species and characterized by wide pereonites 4 (female) or 3 (male), spine-like setae on the posterior margins of pereonites (females), and spine-like setae on the dorsal surface of the pereonites (males). The analyses of *COI* and 18S sequences support the separation of the two species and the recognition of the new genus. Both species feed on bacterial mats and could be found on other specialized habitats, such as wood falls or cold seeps.**

Keywords 18S, bathyal, chemosynthetic environments, CLSM, *COI*, integrative taxonomy, *Jaera*, SEM

Introduction

Isopods are relatively abundant and diverse in soft bottoms in the deep sea in all world oceans (Brandt *et al.* 2005, 2007a, 2018, Kaiser *et al.* 2008, Brix *et al.* 2018a, Schnurr *et al.* 2018, Malyutina and Brandt 2020, Brandt 2022, Kürzel *et al.* 2023, Pereira *et al.* 2025) and new deep-sea isopod species are regularly described (e.g. Brandt *et al.* 2007c, Brix *et al.* 2015, 2018a, b, 2020, Pereira and Doti 2017, Bober *et al.* 2018, Pereira *et al.* 2019, 2020a, 2021, 2023). The suborder Asellota Latreille, 1802 is the most common deep-sea isopod taxon. Asellote isopods can show wide bathymetric ranges of over 1000 m such as *Chelator insignis* (Hansen, 1916) around

Received: 10 November 2025. **Revised:** 15 September 2026. **Accepted:** 1 October 2026
[Version of Record, first published online 19 November 2026, with fixed content and layout in compliance with Art. 8.1.3.2 ICZN. https://zoobank.org/4B875B85-4661-48F6-BC22-72BF523DF3B5]
© The Author(s) 2026. Published by Oxford University Press on behalf of The Linnean Society of London.
This is an Open Access article distributed under the terms of the Creative Commons Attribution License (https://creativecommons.org/licenses/by/4.0/), which permits unrestricted reuse, distribution, and reproduction in any medium, provided the original work is properly cited.

Downloaded from academic.oup.com/zoolinnean/article/208/3/zlag181/9097109 by Natural Environment Research Council user on 24 November 2026

Iceland (Brix *et al.* 2014), but for others depth is a distribution barrier (Brix *et al.* 2014, Knauber *et al.* 2022) depending on the locomotion abilities of the adult stages (Macheriotou *et al.* 2025). Thus, asellote isopod species differ between shallow water and the deep sea (Brandt *et al.* 2007a–c, Brix *et al.* 2018a).

Interestingly, isopods are rarely found at deep-sea hydrothermal vent sites, although peracarids such as amphipods have been reported from geothermal sites (Tandberg *et al.* 2012, 2018). Especially asellote isopods are difficult to be recorded photographically due to their small size (few mm to 20 mm). However, even in vent regions with soft bottoms only a few asellote isopods have been sampled (Wolff 2005). It is unclear why isopods should be less abundant at vent fields compared to soft bottoms in the deep sea given their remarkable adaptive potential (Hessler and Thistle 1975).

Janiridae are considered basal within asellote phylogeny and a typical shallow-water family, but some deep-sea species are known (Hessler *et al.* 1979). The family is polyphyletic (Raupach *et al.* 2009) and needs taxonomic revision (Wilson and Wägele 1994).

Of the 18 *Jaera* species, 17 occur in the northern hemisphere. The only known exception is *Jaera tyleri* Brandt and Malyutina in Linse *et al.*, 2014, found from a whale fall in the Southern Ocean (SO) at 1445 m depth (Linse *et al.* 2014). Contrary to the original diagnosis of the genus *Jaera*, this species lacks eyes and shows differences in the overall body shape, and the triangular shape of the medial lobe of male pleopod I. Despite the morphological difference, the authors did place it into the genus *Jaera* due to many shared characters discussed in Linse *et al.* (2014).

In the present contribution, we erect the new janirid genus ***Bathyjaera*** Kohlenbach and Linse **gen. nov.**, including the description of ***B. giselae*** Kohlenbach and Pereira **sp. nov.** from the Jøtul vent field and the Amundsen Basin in the Arctic Ocean (AO) collected at 3016–4156 m depth. Through an integrative approach, the taxonomic position of *J. tyleri* is revised. In addition, the feeding mechanism of *Bathyjaera* Kohlenbach and Linse gen. nov. species is discussed.

Materials and methods

Study area

The Jøtul vent field was discovered in 2022 (Bohrmann *et al.* 2024) and sits on the ultraslow spreading Arctic Mid-Ocean Ridge (AMOR, Fig. 1) north of the Lucky Strike vent field and south of Svalbard.

The Jøtul vent field consists of the Yggdrasil and the Nidhogg vent sides (Fig. 2), a black smoker, and a shimmering water side (Bohrmann *et al.* 2024). In addition, a new, unnamed, black smoking chimney was discovered by the Ocean Census Arctic Deep Expedition (Rogers *et al.* 2024).

The Amundsen and Nansen Basins, separated by the Gakkel Ridge, are referred to as the Eurasian part of the AO. The Amundsen Basin is characterized by a lower nutrient input, stronger stratification and higher ice cover than the Nansen Basin leading to an increase in small-sized phytoplankton and lower faunal biomass and abundance (Bluhm *et al.* 2015, Kohlbach *et al.* 2025). To the west it is separated by the Lomonosov Ridge from the Amerasian part of the central AO. Up until now, no chemosynthetic habitats have been reported from the Amundsen Basin, except for some hydrothermal vents along the Gakkel Ridge (Fig. 1).

Sampling and sample treatment

During the Ocean Census Arctic Deep Expedition on RV *Kronprins Haakon*, the Jøtul vent field was investigated using the ROV *Aurora*. Specimens of the new species were sampled using the suction sampler during ROV *Aurora*'s dive 11 (77° 26.358′N, 07° 42.132′E) at 3016 m depth at the Nidhogg chimneys (Fig. 2) (Rogers *et al.* 2024).

The sample was sieved through a 250-µm sieve, visible isopods and large mineral precipitate pieces were picked, and the remaining bulk sediment was fixed in 96% ethanol and stored at –20°C (Rogers *et al.* 2024).

During the ArcWatch expedition, seafloor samples were collected using an epibenthic sledge (EBS; Brenke 2005) at station 4 (82° 53.679′N, 130° 10.24098′E) in 4156 m depth (Boetius and Bienhold 2024). On deck, samples were sieved over 300-µm with filtered, cold seawater, bulk-fixed in pre-cooled 96% ethanol, and stored for at least 48 h at –20°C to prevent DNA degradation.

All samples were sorted afterwards at the laboratory using stereomicroscopes.

Morphological drawings

Specimens were stained in Chlorazol Black E® for around 1 h and then transferred into glycerin. Appendages were dissected and temporarily mounted in glycerin for their examination under microscope. The whole specimens, as well as the dissected appendages, were drawn using a Leica DM 2500 microscope with an attached *camera lucida*. Pencil drawings were digitalized with INKSCAPE 1.3.2. After drawing, the appendages were placed in separate microtubes filled with 96% ethanol and are stored with the dissected specimen at the University of Tromsø (UiT) and the Senckenberg Research Institute and Natural History Museum Frankfurt (see Table 1).

Measurements were based on Hessler (1970). The total body length was measured from the clypeus tip to the posterior tip of the pleotelson in dorsal view as outlined in Linse *et al.* (2014). Body parts follow Wilson (1989), whereas Roman numerals were used for appendages following Wolff (1962) and Hessler (1970). Setae were named after Hessler (1970) and Riehl and Brandt (2010).

Imaging methods

Stereomicroscope images of isopod specimens on minerals of the Nidhogg chimney (Fig. 3) were taken with an AmScope MU1803 USB 18.0MP camera connected to a Motic stereomicroscope at the Geological Institute in Tromsø.

Confocal laser scanning microscopy

Two adult specimens of *B. giselae* Kohlenbach and Pereira sp. nov. (one ovigerous female SMF 58539 and one male SMF

Downloaded from academic.oup.com/zoolinnean/article/208/3/zlag181/9097109 by Natural Environment Research Council user on 24 November 2026

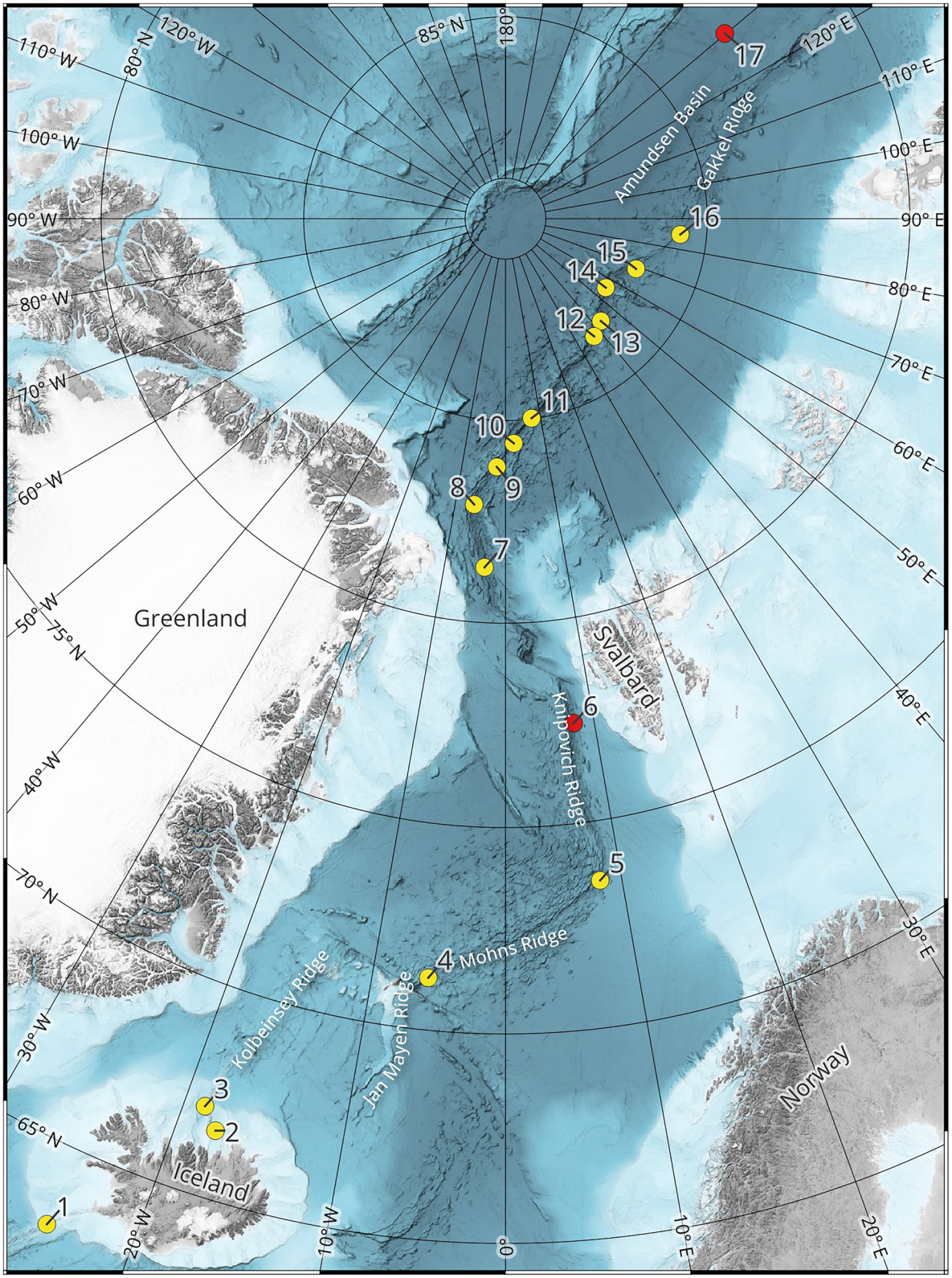

Figure 1 Map showing active hydrothermal vent fields (yellow, 1–5 & 7–16) and sampling sites of *Bathyjaera giselae* Kohlenbach and Pereira sp. nov. (red, 6 & 17) in the Arctic Ocean based on coordinates in Supplementary Table S1: 1 = Steinahóll, 2 = Grimsey, 3 = Kolbeinsey, 4 = Jan Mayen, Soria Moria, Troll Wall, 5 = Loki's Castle, 6 = Jøtul, 7 = Lucky B, 8 = Aurora, 9–16 = active, inferred vents, 17 = sampling site of (SMF 58547) in the central Arctic Ocean. Map made with QGIS v.3.34.0.

Downloaded from academic.oup.com/zoolinnean/article/208/3/zlag181/9097109 by Natural Environment Research Council user on 24 November 2026

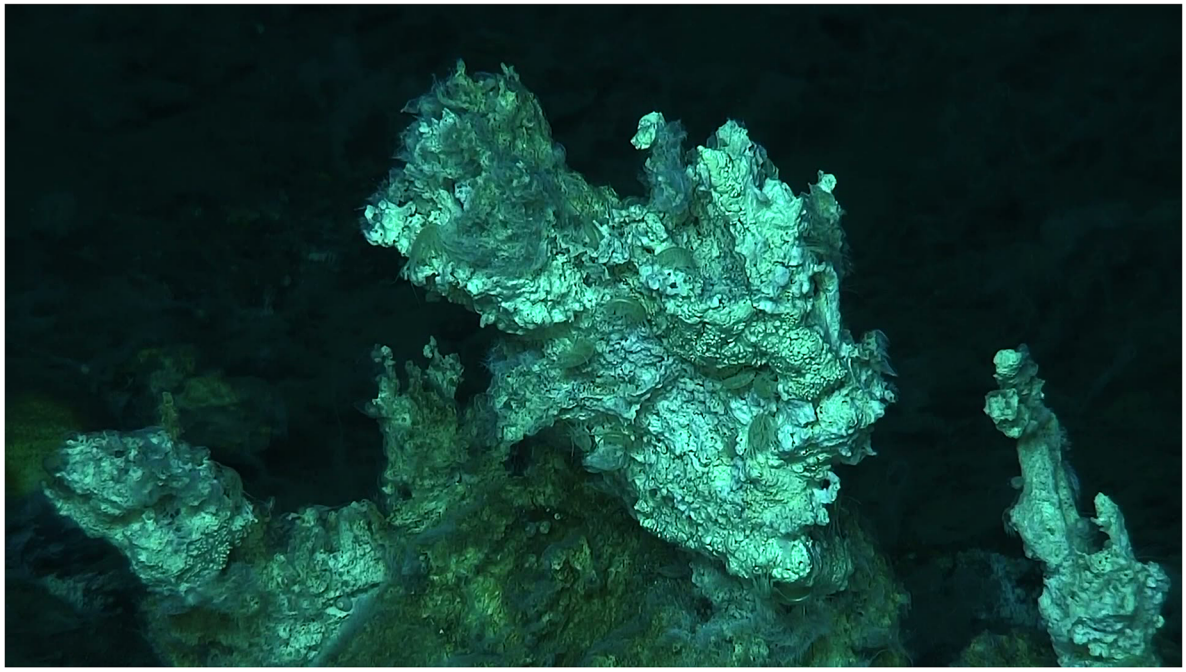

Figure 2 *In situ* image from active venting chimneys hosting the new species at the Nidhogg site taken by ROV *Aurora*.

58540) were used for confocal laser scanning microscopy (CLSM) pictures. Both specimens were stained with Congo red and acid fuchsin, using procedures adapted from Michels and Büntzow (2010). The whole specimens were temporarily mounted on to slides with glycerin, and self-adhesive plastic reinforcement rings were used to support the coverslip (Kihara and da Rocha 2009). The material was examined using a Leica TCS SPV equipped with a Leica DM5000 B upright microscope and three visible-light lasers (DPSS 10 mW 561 nm; HeNe 10 mW 633 nm; Ar 100 mW 458, 476, 488, and 514 nm), combined with the software LAS AF 2.2.1 (Leica Application Suite, Advanced Fluorescence). Images were obtained using an objective HCX PL APO CS 10.0 × 0.40 DRY UV, among 468–633 nm detected emission wavelength, with an acousto-optic tunable filter (AOTF) and an excitation beam splitter TD 488/561/633. A series of stacks were obtained, collecting overlapping optical sections throughout the whole preparation, with an optimal number of sections chosen according to the software. The acquisition resolution was 2048 × 2048 pixels, final images were obtained by maximum projection, and CLSM illustrations were composed from parts and adjusted for contrast and brightness using the software ADOBE PHOTOSHOP C2020.

Scanning electron microcopy

Five specimens of *B. giselae* Kohlenbach and Pereira sp. nov. were used for the scanning electron microscope (SEM): three adult females (TSZCr-19239 and 19240; SMF 58541), one adult male (TSZCr-19241) and one juvenile male (SMF 58541). These specimens were air-dried, mounted using double adhesive carbon stubs, and sputter-coated with carbon with a Leica EM ACE 600. The SEM pictures were taken with an LEO1525 SEM from Zeiss at the University Hamburg in the Zoology Department. One manca (SMF 58541) was mounted but not used for the scanning electron microscopy because of issues during the drying process.

Map

The map (Fig. 1) was composed in QGIS v.3.34.0. The background map is a composition of GEBCO (GEBCO Bathymetric Compilation Group 2024), GLIMS (GLIMS Consortium 2005), IBCAO (Jakobsson *et al.* 2020), and GIMP (Howat 2017), and was created by Simon Dreutter as AWI Basemap. The GEBCO Gazetteer (IHO-IOC GEBCO Gazetteer of Undersea Feature Names) was used for the naming of sea features. Coordinates are listed in Supplementary Table S1.

Molecular methods

The mitochondrial markers cytochrome *c* oxidase subunit 1 (*COI*) and the complete region and a partial region nuclear marker 18S ribosomal RNA gene (18S rDNA) were sequenced for *B. giselae* Kohlenbach and Pereira sp. nov. and *B. tyleri* comb. nov., respectively. Genomic DNA was extracted from dissected pereopods with the NucleoSpin Tissue Kit from Macherey-Nagel (Bioanalysis, Düren, Germany) for *B. giselae* Kohlenbach and Pereira sp. nov., and with the DNeasy Tissue Extraction Kit (Qiagen, Crawley, West Sussex, United Kingdom) for *B. tyleri* comb. nov. following the manufacturer's recommendations. For the *COI* amplification, the LCO1490-JJ/HCO2198-JJ or LCO1490/HCO2198 primers (Table 2) were used.

A thorough description of the polymerase chain reaction (PCR) process can be found in the Supplementary Information under Supporting_Information_PCR.

In addition, three whole specimens of *B. giselae* Kohlenbach and Pereira sp. nov. were used for 18S sequencing. Extraction was done as described above. For the 18S amplification, the sequences were amplified as partially overlapping

Downloaded from academic.oup.com/zoolinnean/article/208/3/zlag181/9097109 by Natural Environment Research Council user on 24 November 2026

Table 1 ***Bathyjaera giselae*** Kohlenbach and Pereira sp. nov. type information and collection numbers. Holotype and paratypes were not used for DNA barcoding. The dash indicates where the information was not applicable.

Type status	Sex/stage	Collection number	BOLD number	Marker gene
Holotype	Female/Ovigerous	TSZCr-19236	–	–
Paratype	Female/Ovigerous	SMF 58538	–	–
Paratype	Male/Adult	TSZCr-19237	–	–
Additional material: CLSM	Female/Adult	SMF 58539	–	–
Additional material: CLSM	Male/Adult	SMF 58540	–	–
Additional material: SEM	Female/Adult	TSZCr-19239	–	–
Additional material: SEM	Female/Adult	TSZCr-19240	–	–
Additional material: SEM	Male/Adult	TSZCr-19241	–	–
Additional material: SEM	Female/Adult	SMF 58541	–	–
Additional material: SEM	Male/Juvenile	SMF 58541	–	–
Additional material: SEM	Manca	SMF 58541	–	–
Additional material	Female/Ovigerous	TSZCr-19238	–	–
Additional material	Female/Ovigerous	TSZCr-19253	–	–
Additional material	37 Females	TSZCr-19254	–	–
Additional material	16 Broken specimens	TSZCr-19255	–	–
Additional material	10 Males	TSZCr-19256	–	–
Additional material	3 Females/Ovigerous	TSZCr-19257	–	–
Additional material	17 Mancas	TSZCr-19258	–	–
Additional material	7 Females	TSZCr-19259	–	–
Additional material	5 Females, 5 Males	TSZCr-19260	–	–
Additional material	2 Females/Ovigerous	TSZCr-19261	–	–
Additional material	18 Females, 9 Males, 17 Mancas	TSZCr-19262	–	–
Additional material	4 Females, 3 Males, 2 Mancas	TSZCr-19242	–	–
Voucher	Female/Ovigerous	TSZCr-19243	BAJAE001-26	*COI*
Voucher	Female/Adult	TSZCr-19244	BAJAE002-26	*COI*
Voucher	Female/Adult	TSZCr-19245	–	–
Voucher	Female/Adult	SMF 58543	–	–
Voucher	Female/Adult	SMF 58544	BAJAE003-26	*COI*
Voucher	Male/Adult	TSZCr-19246	–	–
Voucher	Male/Adult	TSZCr-19247	BAJAE004-26	*COI*
Voucher	Male/Adult	TSZCr-19248	–	–
Voucher	Male/Adult	SMF 58545	BAJAE005-26	*COI*
Voucher	Male/Adult	SMF 58546	BAJAE006-26	*COI*
Voucher 707 (animal gone)	n/a	–	BAJAE008-26	18S
Voucher 709 (animal gone)	n/a	–	BAJAE009-26	18S
Voucher 710 (animal gone)	n/a	–	BAJAE010-26	18S
Additional material	Male/Adult	SMF 58547	BAJAE007-26	*COI*

CLSM, confocal laser scanning microscopy; SEM, scanning electron microscopy.

fragments using four primer pairs: 18S_400F/18S_1155R, 18S_700F/18S_1500R, 18A1_mod/18S_700R, 18A00R_mod/18S_1000F (Table 2).

Successful amplification was assessed via gel electrophoresis (1% agarose gels in Tris-acetate-EDTA buffer with ethidium bromide). For purification ExoSAP-IT PCR Product Cleanup Reagent (Thermo Fisher Scientific™) was used. Samples were put on a thermal cycler at 37°C for 30 min (15 min incubation, 15 min enzyme inactivation). Sequencing of PCR products from *B. giselae* Kohlenbach and Pereira sp. nov. was performed at Macrogen Europe Inc. (Amsterdam, the Netherlands) and for *B. tyleri* comb. nov. at LGC Berlin, Germany.

The obtained sequencing reads were assembled, checked for quality, trimmed, and loaded into GENEIOUS PRIME® 2025.2.1 (Biomatters, Auckland, New Zealand; Kearse *et al.* 2012). The assembled contigs were aligned with sequences from other *Jaera* spp. extracted from NCBI Genbank (Supplementary Table S2), as well as sequences from the munnopsid isopod *Acanthocope galatheae* Wolff, 1962 for the

Downloaded from academic.oup.com/zoolinnean/article/208/3/zlag181/9097109 by Natural Environment Research Council user on 24 November 2026

Table 2 DNA sequencing primers for *COI* and 18S.

Primer name	Sequence [5′–3′]	Reference
LCOJJ (*COI*)	CHACWAAYCATAAAGATATYGG	Astrin and Stüben (2008)
HCOJJ (*COI*)	AWACTTCVGGRTGVCCAAARAATCA	Astrin and Stüben (2008)
LCO1490 (*COI*)	GGTCAACAAATCATAAAGATATTGG	Folmer *et al.* (1994)
HCO2198 (*COI*)	TAAACTTCAGGGTGACCAAAAAATCA	Folmer *et al.* (1994)
18S_400F	ACGGGTAACGGGGAATCAGGG	Dreyer and Wägele (2001)
18S_1155R	GTGAAACTTAAAGGAATTGACGG	Dreyer and Wägele (2001)
18S_700F	GTCTGGTGCCAGCCGCG	Dreyer and Wägele (2001)
18S_1500R	CATCTACGGCATCACAGA	Dreyer and Wägele (2001)
18A1_mod	CTGGTTGATCCTGCCAGTCATATGC	Raupach *et al.* (2009)
18S_700R	CGCGGCTGCTGGCACCAGCAC	Dreyer and Wägele (2001)
18A00R_mod	GATCCTTCCGCAGGTTCACCTACG	Raupach *et al.* (2009)
18S_1000F	CGATCAGATACCGCCCTAGTTC	Dreyer and Wägele (2001)
SSUA NSF4 (18S)	CTGGTTGATYCTGCCAGT	Hendriks *et al.* (1989)
SSUA NSR581 (18S)	ATTACCGCGGCTGCTGGC	Wilmotte *et al.* (1993)

COI and 18S alignment as the outgroup using using MAFFT v.7.526 (Katoh *et al.* 2019). The *COI* alignment was additionally checked for the correct reading frame and internal stop codons. The best-fit evolutionary models were estimated for each loci using IQ-TREE v.2.3.6 (Minh *et al.* 2020) according to the Bayesian information criterion (Schwarz 1978), and the closest implementations in MrBayes v.3.2.7a (Altekar *et al.* 2004, Ronquist *et al.* 2012) were applied to perform the Bayesian evolutionary analysis. The two loci were analysed separately using the same MCMCMC (metropolis-coupled Markov chain Monte Carlo) settings (10 million generations, four independent runs with one cold and three heated chains each, sampled every 1000 generations), with a partitioning scheme that allowed divergent substitution rates across codon sites applied to the *COI* analysis. Convergence of the parallel runs was examined in TRACER v.1.7.2 (Rambaut *et al.* 2018), and the 50% majority-rule consensus tree was generated by discarding the first 25% of the sampled trees as burn-in. The resulting trees were rerooted and visualized in R (v.4.5.0, R Development Core Team 2021, Posit Team 2025) using packages TIDYVERSE (v.2.0.0; Wickham *et al.* 2019), APE (v.5.8-1; Paradis and Schliep 2019), TREEIO (v.1.34.0; Wang *et al.* 2020), and GGTREE (v.4.1.1, Yu *et al.* 2017). Genetic pairwise distance was calculated using the standard uncorrected *p*-distances assuming uniform and homogenous rates with pairwise deletion of gapped positions in MEGA12 (Supplementary Table S3) (Stecher *et al.* 2020, Kumar *et al.* 2024).

Voucher information, taxonomic classifications, and sequences for both species are accessible through the public dataset 'BAJAE' on the Barcode of Life Data Systems (BoLD; www.boldsystems.org) Table 1.

Results

Taxonomy

Family Janiridae G.O.Sars, 1897

Genus Bathyjaera Kohlenbach and Linse gen. nov.

ZooBank registration: https://zoobank.org/48890C9B-C674-4250-8431-3F7659BDCFDC

Synonyms: None.

Type species: ***Bathyjaera giselae*** Kohlenbach and Pereira **sp. nov.**; here designated.

ZooBank registration: https://zoobank.org/4B875B85-4661-48F6-BC22-72BF523DF3B5

Species included: Bathyjaera tyleri (Brandt and Malyutina, 2014) comb. nov. and *Bathyjaera giselae* Kohlenbach and Pereira sp. nov.

Diagnosis: Body wide, body length/width ratio at pereonite 1 1.6–2.0. Head without eyes. Clypeus apically concave. Pereonites lateral margins convex, with spine-like setae; coxae not visible in dorsal view. Pereonite 5 shortest, length 0.5–0.7 pereonite 1 length. Pleotelson with medial projection in uropod notch. Uropod, rami tips not reaching outline of pleotelson from the notch. Antennula flagellum with two or three articles. Antenna short, less than half of body length; article 1 shortest, exopod on article 3 absent. Pereopod I ambulatory, dactylus with two claws and robust setae. Pereopods II–VII also ambulatory, dactylus with three claws, dorsal claw twice longer than ventral claw. Male, pleopod I length less than 0.6 pleotelson length, medial lobe triangular; pleopod III opercular.

Distribution: Chemosynthetic environments at 1445–4156 m depth (Fig. 4).

Etymology: Bathyjaera Kohlenbach and Linse gen. nov. (Latin, female) is named after its depth distribution and its resemblance with *Jaera* species.

Generic remarks: Species of *Bathyjaera* Kohlenbach and Linse gen. nov. resemble species of *Jaera* but differ from those by (characters of *Jaera* between parentheses, Table 3): body wide

Downloaded from academic.oup.com/zoolinnean/article/208/3/zlag181/9097109 by Natural Environment Research Council user on 24 November 2026

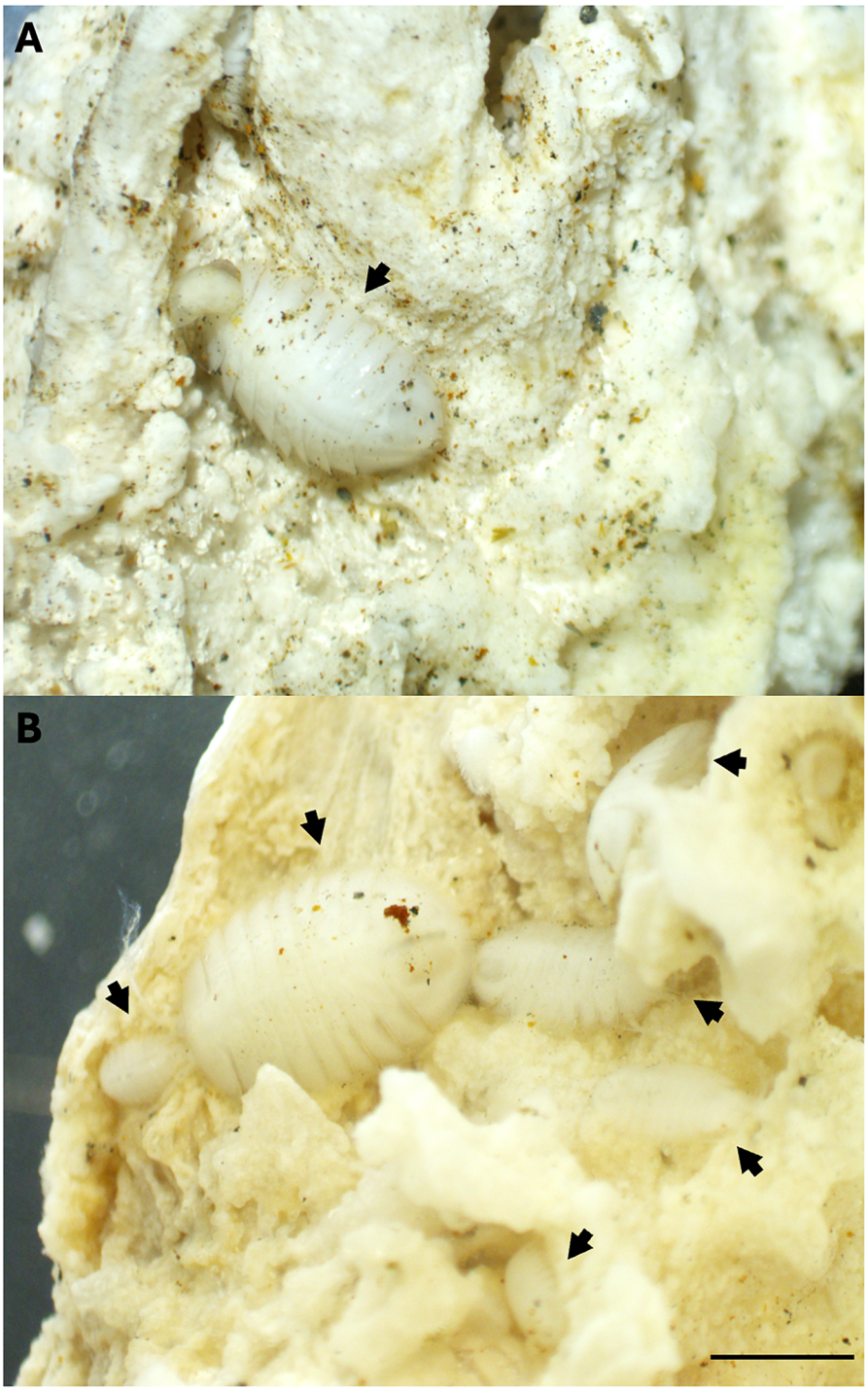

Figure 3 *Bathyjaera giselae* Kohlenbach and Pereira sp. nov. sitting on vent precipitate. Pictures taken in the laboratory. Scale = 1 mm, only for picture B. Arrows indicate specimens.

(narrow), the antenna and pleopods I shorter (longer), the shape of the medial lobe of the pleopods I triangular (broad), pereopods II–VII with a small ventral claw on their dactylus (large ventral claw), the uropod exopod and endopod are equally long (endopod longer than exopod), a medial projection present in the caudal notch in the pleotelson (medial projection absent) and the pleotelson itself wider (narrower). In addition, all *Bathyjaera* Kohlenbach and Linse gen. nov. species are from chemosynthetic environments, such as whale falls and hydrothermal vents, at 1445–4156 m depth. Linse *et al.* (2014) modified the diagnosis of the genus *Jaera* regarding the presence of eyes in order to fit the description of their new species (*J. tyleri*). In the present contribution, the new blind genus *Bathyjaera* Kohlenbach and Linse gen. nov. is erected. Thus, the modified diagnosis presented by Linse *et al.* (2014) should be omitted.

Downloaded from academic.oup.com/zoolinnean/article/208/3/zlag181/9097109 by Natural Environment Research Council user on 24 November 2026

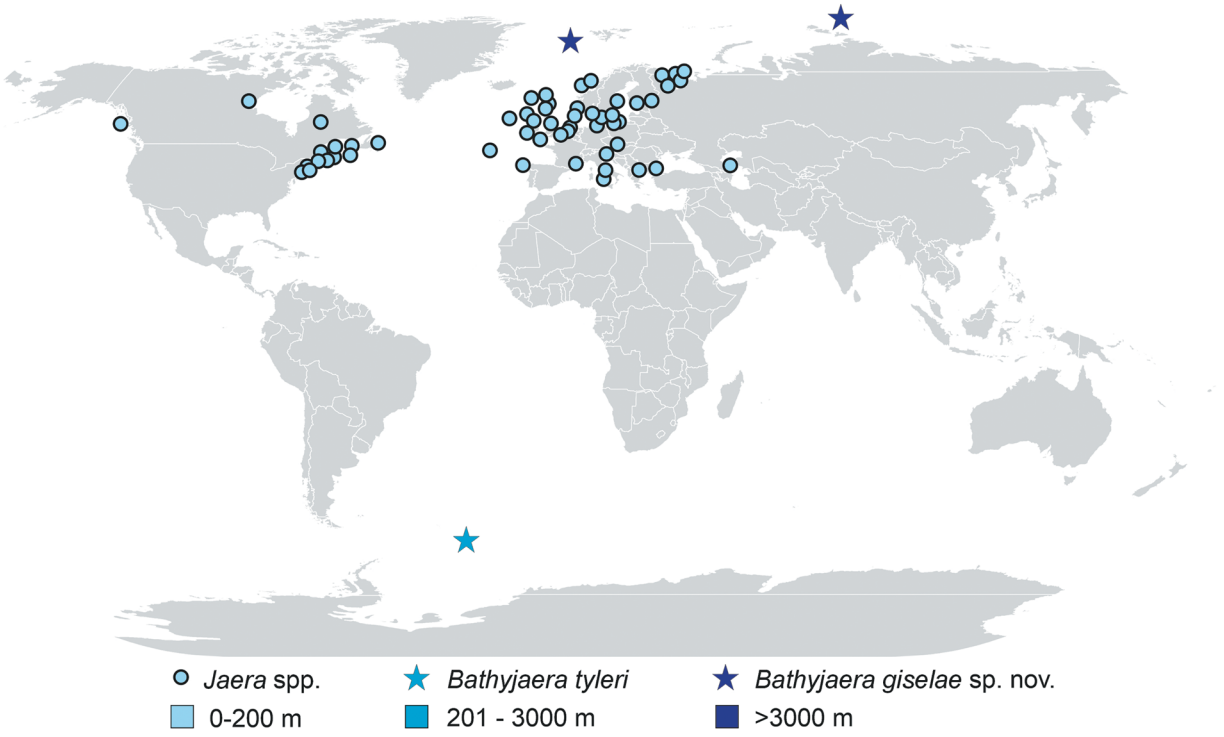

Figure 4 Global map of the distribution of *Jaera* spp. and *Bathyjaera* Kohlenbach and Linse gen. nov. spp.

The general habitus of *Bathyjaera* Kohlenbach and Linse gen. nov. also resembles the habitus of the recently described deep-sea family Basoniscidae Wilson, 2024 from New Zealand (Wilson 2024). Both taxa share the lack of eyes, the clypeus visible dorsally, and the coxae not visible in dorsal view (Table 4). However, the new genus can be distinguished from Basoniscidae by (characters of Basoniscidae between parentheses): antenna less than half of body length (half of body length), mandibular molar process rather circular with sharp denticles (with two distal denticulated ridges), maxilliped palp article 2 wider than long (longer than wide), pereopods I–VII thick and similar in length (pereopods slender, pereopods IV and V shorter than remaining pereopods), pereopods II–VII dactylus with dorsal claw larger than ventral claw (dorsal claw smaller than ventral claw), pleonite 1 free (all pleonites fused), pleopodal III exopod biarticulated (monoarticulated) (as in Janiridae), uropod exopod equal in length to endopod (exopod much shorter than endopod), uropodal insertion in a deep notch (uropods inserted in a shallow notch), anus not covered by the uropods but placed in the pleopodal chamber (anus covered by the uropods), male pleopod I not widening distally (widening distally), lateral lobes well developed (reduced) and medial lobes distinctly projected, subtriangular (medially truncated with a small projection) (Table 4).

Bathyjaera tyleri (Brandt and Malyutina in Linse et al., 2014) comb. nov.

Synonyms: Jaera tyleri Brandt and Malyutina in Linse, Jackson, Malyutina and Brandt, 2014.

Diagnosis [modified from Linse et al. (2014)*]:* Body widest at pereonite 3 (female) or 6 (males). Head, frontal margin smooth, slightly concave. Antenna, subequal in length to head. Maxilliped, basis length 2.7 width; palp length 0.9 basis length. Uropods 0.2 pleotelson length; protopod length 1.25 width; endopod subequal in length to protopod. Male, pleopod I, medial lobes subtriangular, distally rounded, equal in length and 2.0 × as broad as lateral lobes.

Bathyjaera giselae Kohlenbach and Pereira sp. nov.

(Figs 5–15)

Holotype: Ovigerous female (4.04 mm). Vent precipitates, Nidhogg chimney, Jøtul vent field, Arctic Ocean, Ocean Census Arctic Deep Expedition, ROV *Aurora*, dive 11 (77°26.242′N, 07°42.110′E), 3016.5 m, RV *Kronprins Haakon*, 13 May 2024, catalogue number TSZCr-19236 (UiT).

Paratypes: Same data as holotype. The ovigerous female used for dissection of the antennula and antenna, mouthparts, pereopods, and pleopods (Figs 5–8) is deposited as SMF 58538 (Senckenberg). The male drawn (Figs 9 and 10) is deposited as catalogue number TSZCr-19237 (UiT) with the removed appendages.

Additional specimens: Altogether 99 females (1.33–4.26 mm), 38 males (1.52–4.56 mm), and 39 mancas (0.80–1.22 mm). Same data as holotype (catalogue numbers TSZCr-19238, TSZCr-19242–19248 at UiT; SMF 58539–58546 at Senckenberg). The specimens for the CLSM study are deposited as SMF 58539 and 58539 (Figs 11 and 12). The specimens on stubs for the SEM study are deposited as catalogue number TSZCr-19239–19241 and SMF 58541 (Figs 13–15). One male (1.56 mm) from PS138 ArcWatch-1, Amundsen Basin, Station 4 (82° 53.679′N, 130° 10.24098′E), 4156 m, RV *Polarstern*, 24.08.2023, SMF 58547.

Downloaded from academic.oup.com/zoolinnean/article/208/3/zlag181/9097109 by Natural Environment Research Council user on 24 November 2026

Table 3 Comparison between the type species of the genus *Jaera* and the two species of *Bathyjaera* Kohlenbach and Linse gen. nov. f = female, m = male. A dash indicates that the information was not applicable.

	***J. albifrons* (f)**	***J. albifrons* (m)**	***B. tyleri* comb. nov. (f)**	***B. tyleri* comb. nov. (m)**	***B. giselae* sp. nov. (f)**	***B. giselae* sp. nov. (m)**
Body widest	pereonite 5	pereonite 3	pereonite 7	pereonite 6 + 7	pereonite 4	pereonite 3
Body length/width ratio at pereonite 1	2.88	2.48	2.02	1.95	1.55	1.84
Eyes	present	present	absent	absent	absent	absent
Pleotelson, length to width	0.75	0.72	0.53	0.54	0.54	0.61
Caudal notch in uropod incision	absent	absent	present	present	present	present
Caudal notch in iropod incision, medial projection length	–	–	0.3	0.3	0.5	0.5
Antennula length to head	n/a	n/a	subequal	subequal	longer	longer
Antenna, article 1–4	Subequal	subequal	article 1 shortest	article 1 shortest	article 1 shortest	article 1 shortest
Antenna, length to body length	0.8	0.7	0.3	0.3	0.43	0.4
Maxilliped, palp to endite length	n/a	n/a	0.9	0.9	1.1	1.1
Pereopods II–VII, dactylus, length ventral claw to dorsal claw	equal	equal	0.5	0.5	0.5	0.5
Pleopods I, length to pleotelson	–	0.83	–	0.59	–	0.52
Pleopod I, shape of medial lobe	–	broad edge, turned sideways	–	triangular with rounded tip, straight	–	triangular with rounded tip, straight
Pleopod I, medial lobe width to lateral lobe width	–	n/a	–	2.0	–	3.5
Uropod, exopod and endopod length	exopod shorter	exopod shorter	equal	equal	equal	equal
Uropod, protopod length to width	0.87	0.87	equal	equal	1.35	1.35
Depth distribution (m)	0–20	0–20	~1400	~1400	3052–4156	3052–4156

Diagnosis: Body widest at pereonite 4 (females) or 3 (males); pereonites with spine-like setae on lateral and posterior margins (females) or dorsal surface (males). Pleotelson length to width 0.5, width subequal or narrower than pereonite 1 width; medial projection length 0.5 distal margin notch length. Antennula longer than the head. Antenna length 0.3–0.5 body length. Maxilliped, basis length 1.9 width, palp length 1.4 basis length, palp article 2 widest. Uropods 0.2 pleotelson length; protopod length subequal in width; endopod length 0.6 protopod length. Male, pleopod I, medial lobes distally rounded, subequal in length and 3.5× as broad as lateral lobes.

Etymology: Bathyjaera giselae Kohlenbach and Pereira sp. nov. is named after the first author's late maternal grandmother Gisela Bahl.

Description: Female description [habitus based on female holotype (TSZCr-19236); appendages based on female paratype (SMF 58538)].

Body (Figs 5–8, 13–15) length 1.6 width of pereonite 1. Head length 0.2 width; clypeus visible dorsally, protruding between proximal article of antennula, distally convex. Pereonites slightly increasing in width from pereonite 1 to pereonite 4, then decreasing in width; lateral margins slightly rounded, with spine-like setae, longer in medial part of pereonites; posterior margins also with spine-like setae. Pereonite 1 length 1.3 head length, width 1.3 head width; pereonites 1–4 and 6 or 7 almost of same length. Pleotelson length 0.5 width, 0.3 body length, subequal as wide as pereonite 1, terminal notch depth 0.1 pleotelson length, medial projection of the notch 0.5 of notch length. Body outline beside frontal

Downloaded from academic.oup.com/zoolinnean/article/208/3/zlag181/9097109 by Natural Environment Research Council user on 24 November 2026

Table 4 Morphological comparison between Janiridae, Basoniscidae, and *Bathyjaera* Kohlenbach and Linse gen. nov. Character states were extracted from Wilson (1994), Wilson and Wägele (1994), and Wilson (2024).

Character	Janiridae (Wilson 1994, Wilson and Wägele 1994)	Basoniscidae (Wilson 2024)	*Bathyjaera* gen. nov.
Body widest	Either at pereonites 4–5 or 6–7 or pleotelson.	Width similar everywhere.	Either at pereonites 3, 4 or 6.
Head	Wider than long or vice versa.	Broadening posteriorly with separated antennal insertions and lateral margins.	Broadening posteriorly with antennal insertions and convex lateral margins.
Eyes	Present.	Absent.	Absent.
Clypeus visible dorsally	Yes or no.	Yes.	Yes.
Pereion, Coxae, visible dorsally	Yes or no.	No.	No.
Pleon	Pleonite 1 free.	All pleonites merged into pleotelson.	Pleonite 1 free.
Anus	Inside of pleopodal cavity. Not covered by uropods.	Outside of pleopodal cavity. Covered by uropods.	Inside of pleopodal cavity. Not covered by uropods.
Antenna	Longer than half body length.	As long as half body length.	Less than half of body length.
Mandible, molar process	Either truncate, spine-like or distally rounded with several setae.	Cylindrical with two distal ridges of sharp denticles.	Cylindrical, distally with small denticles, without ridges.
Maxilliped, palp article 2 width	Longer than wide or wider than long.	Longer than wide.	Wider than long.
Pereopods I–VII	Similar in length.	Pereopod I shortest; pereopods IV and V shorter than remaining.	Pereopods II–V similar in length; pereopod VI longest.
Pereopods I–VII	Slender.	Slender.	Thick.
Pereopods I–VII, claws	Both claws approximately of the same size, or ventral claw smaller.	Ventral claw more robust than dorsal claw.	Ventral claw half as long as dorsal claw.
Pleopod III, exopod	With two articles or articles fused, longer than endopod or same length as or shorter than endopod.	Uniarticulate, shorter than endopod	With two articles, longer than endopod.
Uropod length	Near that of pleotelson or distinctly shorter than pleotelson or elongate.	Uropods not reaching outline of pleotelson.	Uropods not reaching outline of pleotelson.
Uropod insertion	With a shallow notch for uropod insertion or not.	With shallow notch for uropod insertion.	Deep insertion with caudal projection.
Uropod, exopod	Somewhat shorter than endopod; tiny or rudimentary or absent.	Tiny.	As long as endopod.
Male pleopod I shape	Wide or merged to a 'V'–shape.	Widening distally.	Not widening distally.
Male pleopod I, lateral lobes	Reduced or with distinct lateral lobes.	Reduced.	Distinct lateral lobes.
Male pleopod I, medial lobes	Broad and rounded.	Medially truncate with small distolaterally projecting horn.	Subtriangular.

margin of head and pleotelson notch surrounded with stout setae of alternating lengths (short/long).

Antennula (Fig. 5) length 1.3 head length; article 1 length 1.4 width, with one distomedial stout seta and two or three small distolateral setae, with row of fine setules on lateral and mesial margins; article 2 0.7 length and 0.4 width of article 1, with three or four simple and three broom setae distally, and one or two simple setae medially; article 3 0.5 length of article 2, with one simple seta distally; article 4 0.7 length of article 3, with two broom setae distally and one simple seta laterally; article 5 subequal in length to of article 4, with one aestetasc, one broom, one long simple, and tgree shorter simple setae distally. All articles covered with cuticular combs.

Antenna (Fig. 5) 0.4 body length. Article 1 shortest and narrowest, length 0.2 and width 1.1 of article 6, glabrous; article 2 length 0.4 and width 1.6 of article 6, glabrous; article 3 0.4 length and 2.0 width of article 6, with one stout seta distomedially and two stout setae distolaterally; article 4 0.3 length and 1.5 width of article 6, with five setae

Downloaded from academic.oup.com/zoolinnean/article/208/3/zlag181/9097109 by Natural Environment Research Council user on 24 November 2026

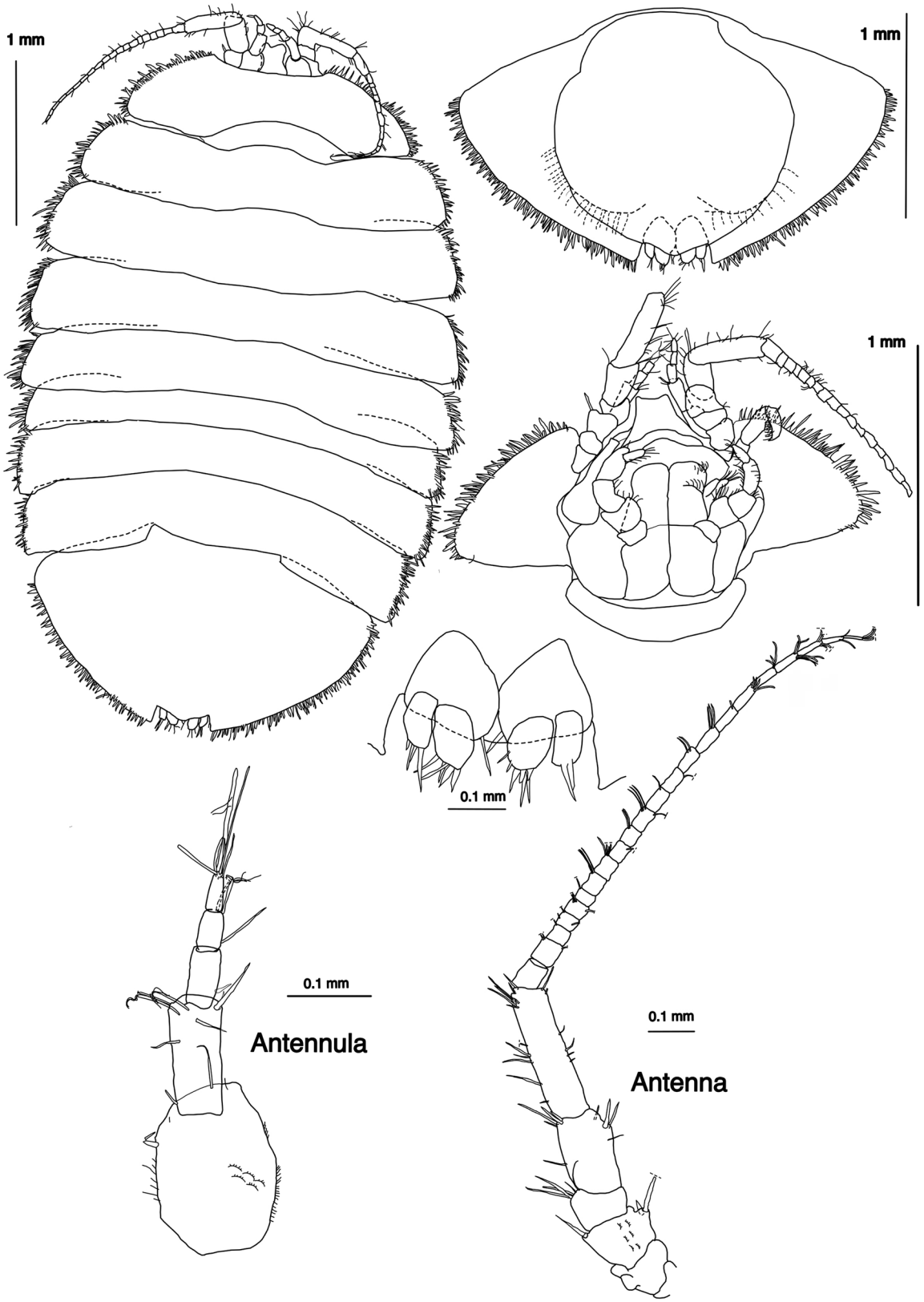

Figure 5 *Bathyjaera giselae* Kohlenbach and Pereira sp. nov. Holotype ovigerous female [TSZCr-19236 (UiT)]. Antennula and antenna from the ovigerous female Paratype [SMF 58538 (Senckenberg)].

Downloaded from academic.oup.com/zoolinnean/article/208/3/zlag181/9097109 by Natural Environment Research Council user on 24 November 2026

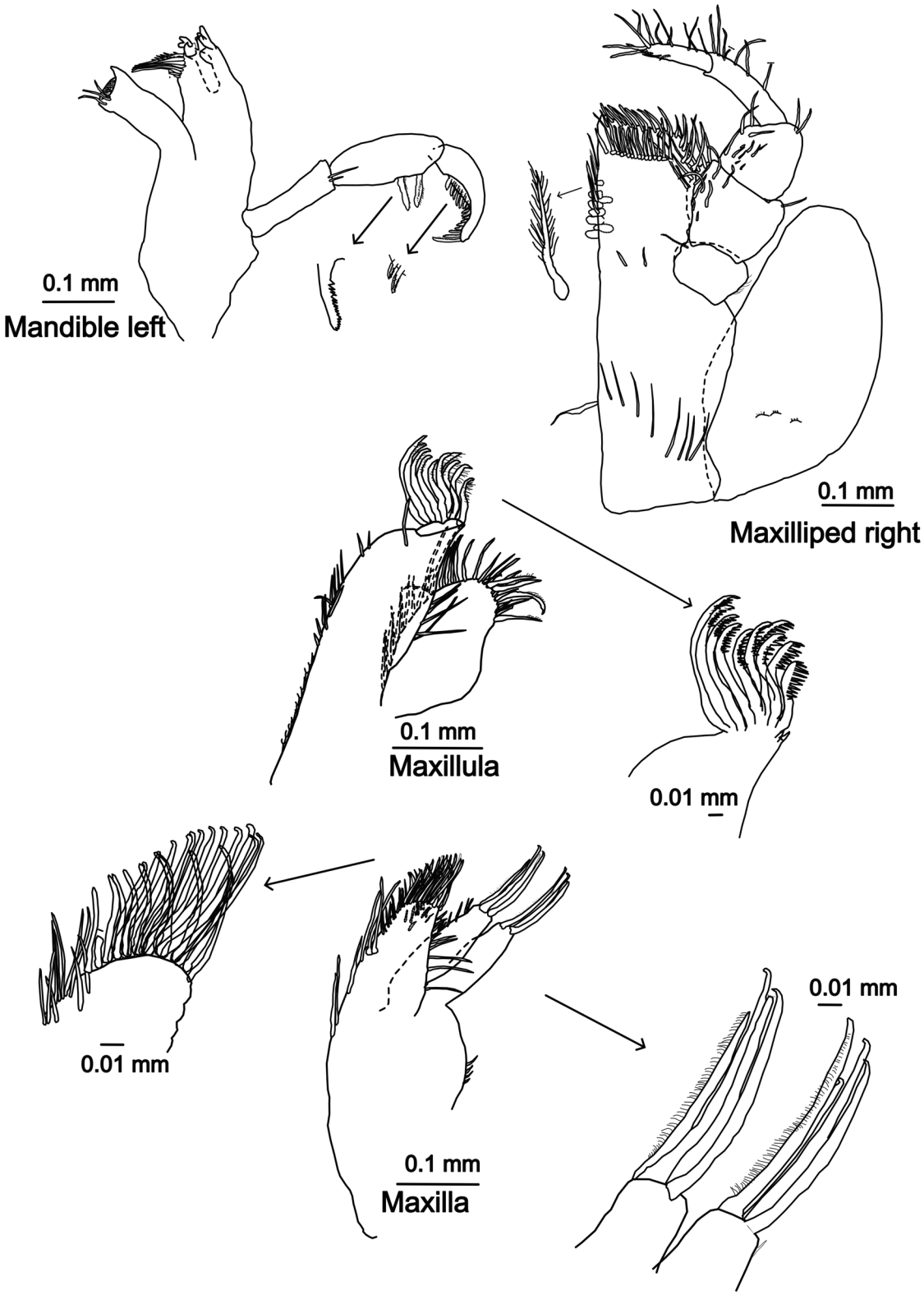

Figure 6 *Bathyjaera giselae* Kohlenbach and Pereira sp. nov. Paratype ovigerous female [SMF 58538 (Senckenberg)]. Mouthparts.

distomedially; article 5 0.6 length and 1.5 width of article 6, with one or two medially, four distomedially, one laterally, and three distolaterally simple setae; article 6 longest, length 3.9 width, with four laterally, six medially, seven distomedially, and two distolaterally simple setae of varying lengths. Flagellum length 1.5 peduncle length, composed by 22 articles, tapering distally; most articles with one to three slender setae distomedially and distolaterally.

Mandible (Fig. 6) incisor process with six distally rounded cusps; spine row with eight to ten spines; molar process 1.1

Downloaded from academic.oup.com/zoolinnean/article/208/3/zlag181/9097109 by Natural Environment Research Council user on 24 November 2026

as long and 0.5 as wide as incisor process, ventral margin of triturative surface with a few denticles and three setae; *lacinia mobilis* of left mandible slightly bent distally, with four teeth, 0.6 length of incisor process. Palp, article 1 0.8 length and 0.7 width of article 2, with two slender setae distally; article 2 longest, length 2.6 width, with two comb-like setae on distal half; article 3 curved, length 0.9 article 2 length, 0.7 as wide as article 2, with a row of stout setulated setae ventrally.

Maxillula (Fig. 6) lateral endite subequal in width to mesial endite, distal margin truncated, with short spine-like setae distomedially and ten to twelve stout curved comb-like setae distally; mesial endite distal margin rounded, with four or five stout setulated setae and a tuft of slender setae.

Maxilla (Fig. 6) mesial endite broadest, lateral endite narrowest, all endites of approximately the same length; mesial endite distal margin truncated, with two rows of stout setae ending with small hooks; lateral and middle endites each with four comb-like distal setae with small hooks.

Maxilliped (Fig. 6) endite length 2.8 width, with two to eight coupling hooks, distal margin straight, with two rows of slender setae curved medially and five setulated setae on the lateral outer margin. Palp length 1.1 endite length; article 1 shortest, length 0.5 and width 2.8 of article 4, with one long simple seta distomedially; article 2 broadest, equal in width to endite width, length 0.9 and width 3.8 of article 4, medial margin slightly convex, with 14 or 15 setae distomedially and one seta distolaterally; article 3 length 0.8 and width 2.7 of article 4, with two setae distolaterally, medial margin slightly convex, with eight or nine setae; article 4 length 3.5 width, with seven to ten setae laterally; article 5 length 0.7 and width 0.7 of article 4, with 14–16 simple setae marginally. Epipod reaching distal margin of palp article 2, twice as long as wide, with rounded lateral margin, and covered with cuticular combs.

Pereopod I (Fig. 7) basis longest article, with three simple setae ventrally and four simple setae dorsally; ischium 0.8 basis length, with five stout setae dorsally and three simple setae ventrally; merus 0.4 basis length, with one long and one short stout seta distoventrally, three stout setae ventrally, two long and two short stout setae distodorsally, and two simple setae medially; carpus 0.7 basis length, with 1 slender and two or three simple setae distodorsally, six simple setae ventrally, ventral margin with fine setules; propodus 0.8 basis length, with one robust seta distoventrally, three to five simple setae ventrally, two slender setae dorsally, and three simple and one stout seta distodorsally, ventral margin with fine setules; dactylus 0.3 basis length, ventral claw 0.5 length of dorsal claw.

Pereopod II (Fig. 7) length 1.2 pereopod I length; length ratios of ischium–dactylus (including dorsal claw) to basis: 0.7, 0.3, 0.6, 0.6, 0.3; basis with three or four simple setae dorsally and five to seven simple setae ventrally; ischium with two or three simple, one robust and one stout seta dorsally, three simple setae ventrally, one simple seta distoventrally and one simple seta medially; merus with three or four stout, one to three robust and one simple seta distodorsally, two or three simple setae ventrally, one simple seta distoventrally and one simple seta medially; carpus width 1.3 pereopod I carpus width, armed with stronger setae than in pereopod I: three simple setae ventrally, one robust, two stout, one broom and two simple setae distodorsally, two or three simple setae distoventrally; propodus with two simple and one robust seta ventrally, one to three simple seta dorsally, three simple setae distodorsally, two simple setae ventrally, one simple seta medially, and one robust and one simple seta distoventrally; dactylus ventral claw 0.5 length of dorsal claw.

Pereopod III (Fig. 7) length equal to pereopod II length, length ratios of ischium–dactylus (including dorsal claw) to basis: 0.7, 0.4, 0.7, 0.6, 0.3; basis with four simple setae ventrally and one simple seta dorsally; ischium with three simple setae and one stout seta dorsally, three simple setae ventrally and one simple seta medially; merus with four to six stout setae distodorsally, two simple setae ventrally, one simple seta distoventrally and one simple seta medially; carpus with three simple setae ventrally, one robust, four or five stout, one broom and one simple seta distodorsally, one simple seta distoventrally, and two simple setae medially; propodus with three simple setae ventrally, one robust seta distoventrally, two simple setae dorsally, two slender, and one broom seta distodorsally, and one slender seta medially; dactylus ventral claw 0.6 length of dorsal claw.

Pereopod IV (Fig. 7) as long as pereopods II and III, length ratios of ischium–dactylus (including dorsal claw) to basis: 0.7, 0.4, 0.7, 0.8, 0.3; dorsal setae on ischium stronger than those on pereopods II, III, VI, and VII; basis with three simple setae dorsally, four to seven simple setae ventrally, and simple seta distoventrally; ischium with three simple setae ventrally, two simple setae medially, one simple seta dorsally, and one or two simple and two stout setae distodorsally; merus with one or two simple setae distoventrally setae, two simple setae ventrally, three simple setae medially, and two robust, two to four stout, and one simple seta distodorsally; carpus with two robust, two stout, one simple, and one broom seta distodorsally, one simple setae distoventrally, one simple seta medially, and three simple setae ventrally; propodus with three or four simple setae ventrally, one robust seta distoventrally, two to four simple and one broom seta distodorsally, and two simple setae dorsally; dactylus ventral claw 0.5 length of dorsal claw.

Pereopod V (Fig. 7) length equal to pereopod IV length, length ratios of ischium–dactylus to basis: 0.7, 0.3, 0.6, 0.6, 0.4; dorsal setae on ischium stronger as strong as on pereopods IV; basis with one simple seta dorsoventrally, two to four simple setae ventrally, and three simple setae dorsally; ischium with three or four simple setae ventrally, two simple setae dorsally, and three stout setae distodorsally; merus with two simple setae distoventrally, one or two simple setae ventrally, and five stout setae distodorsally; carpus with two robust, three stout, and one broom seta distodorsally, two distoventral, four ventral, and one medial simple setae; propodus with two to four ventral setae, one robust seta distoventrally, four simple setae dorsally, and three simple and one broom seta distodorsally; dactylus ventral claw 0.5 length of dorsal claw.

Pereopod VI (Fig. 7) longest pereopod, length 1.1 pereopod V length, length ratios of ischium–dactylus to basis: 0.6, 0.3, 0.6, 0.6, 0.3; basis with five or six simple setae dorsally and

Downloaded from academic.oup.com/zoolinnean/article/208/3/zlag181/9097109 by Natural Environment Research Council user on 24 November 2026

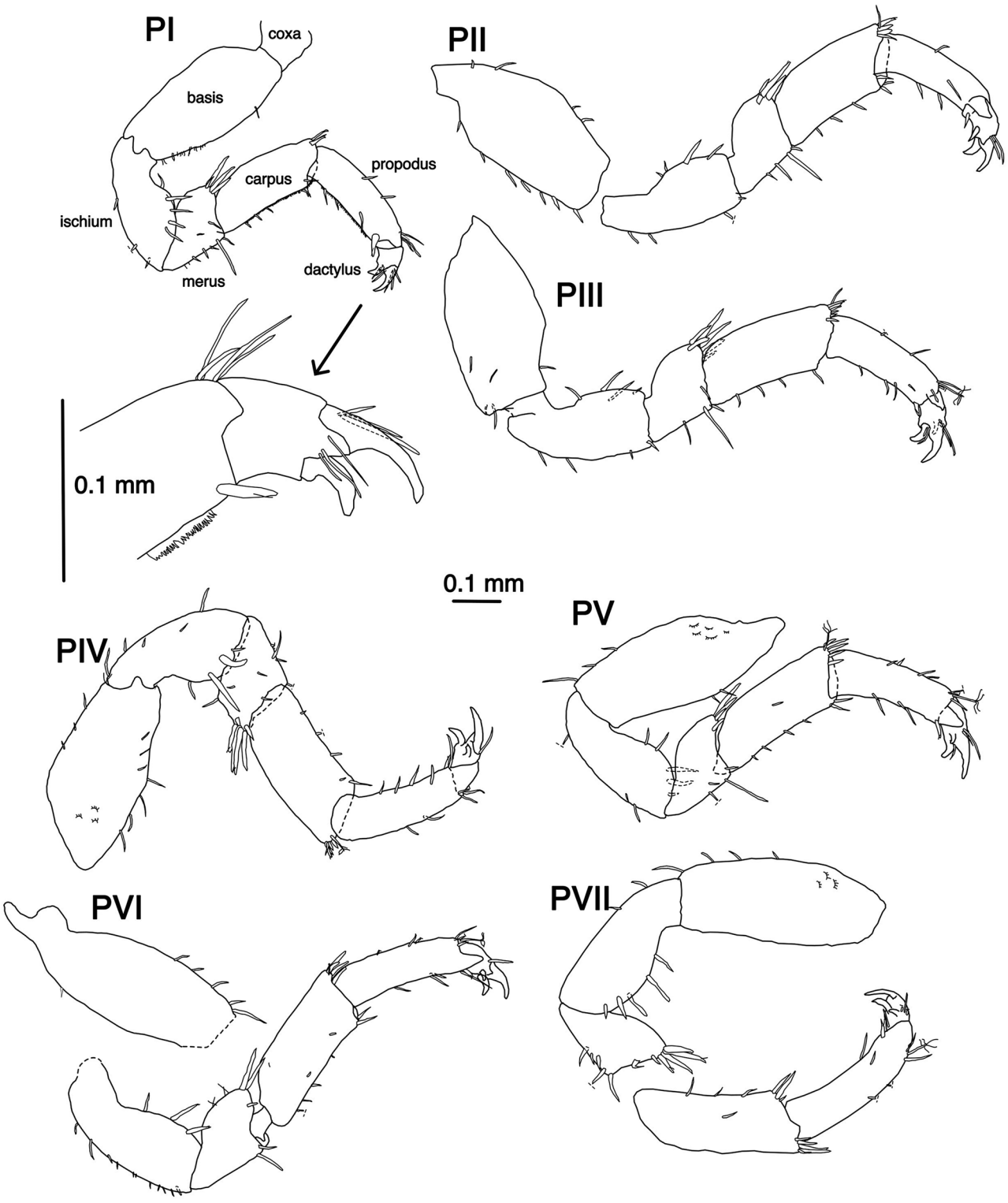

Figure 7 *Bathyjaera giselae* Kohlenbach and Pereira sp. nov. Paratype female [SMF 58538 (Senckenberg)]. Pereopods I–VII. P = pereopod. All pereopods share the same scale bar.

one to three simple setae ventrally; ischium with two robust and one or two stout setae dorsally, three stout setae distodorsally, 11 simple setae ventrally, and three simple setae medially; merus with two or three simple distoventral setae, one stout seta ventrally, one simple seta medially, three robust, one stout, and one simple seta distodorsally; carpus with four to six stout and one simple seta distodorsally, two simple setae distoventrally, three simple setae ventrally, and two simple setae medially; propodus with two or three setae ventrally, one robust and one simple seta distoventrally, three simple setae dorsally, and two or three simple setae and one broom seta distodorsally, dactylus ventral claw 0.6 length of dorsal claw.

Downloaded from academic.oup.com/zoolinnean/article/208/3/zlag181/9097109 by Natural Environment Research Council user on 24 November 2026

Pereopod VII (Fig. 7) length 0.9 pereopod VI length, length ratios of ischium–dactylus to basis: 0.8, 0.4, 0.7, 0.8, 0.3; basis with three or four simple setae ventrally, one simple seta distoventrally, and four simple setae dorsally; ischium with two to five simple setae ventrally; one or two stout, one robust and one simple seta dorsally, two stout, two robust, and one or two simple setae distodorsally; merus with one simple and one stout seta distoventrally, two simple and one or two stout setae ventrally, and two or three stout, two or three robust, and one simple setae distodorsally; carpus with three stout and one or two robust setae distoventrally, three to five simple setae ventrally, two or three stout setae distodorsally, and one or two medial setae; propodus with one simple seta ventrally, one robust seta distoventrally, one simple seta medially, two to four simple setae dorsally, and two simple and one broom seta distodorsally, dactylus ventral claw 0.6 length of dorsal claw.

Pleopod II (Fig. 8) opercular, round, flat, covering anus, laterally and distally fringed with 64 simple setae, simple setae on dorsal surface.

Pleopod III (Fig. 8) 0.7 of pleopod II length, protopod and endopod as long as exopod; endopod length 1.1 protopod length, without any setae; exopod 2.4 as long as wide, 1.8 as long as endopod, laterally and distally fringed with simple setae, distal article 0.7 as long and 0.8 as wide as proximal article.

Pleopod IV (Fig. 8) protopod length 0.9 width, endopod 1.9 exopod width and 0.4 exopod length; exopod width 0.2 length, with short setules on margins.

Pleopod V (Fig. 8) one lobe, length 1.7 width.

Uropod (Fig. 5) length 0.2 pleotelson length. Protopod equal in length to width, with one or two long setae on small distomedial projection; endopod 0.6 length and 0.5 width of protopod, with three to seven long setae distally; exopod equal in length and 0.7 width of endopod, with one to four simple setae distally.

Male description (based on paratype male TSZCr-19237). As female except for:

Body (Figs 9–12, 14,15) length 1.8 width of pereonite 1. Pereonites slightly increasing in width until pereonite 3, then decreasing in width. Dorsal surface with spine-like setae. Pereonite 1 equal in length to head. Pleotelson length 0.6 width, medial projection of the notch 0.4 of notch length.

Pleopod I (Fig. 10) length 1.5 proximal width, and 3.4 midlength width; with three or four simple setae on distal ventral surface, row of eight simple setae around distolateral lobe; distolateral lobes slender (length to midlength width 4.4), projected laterally; medial lobes subtriangular, with rounded tip, subequal in length and 3.5× as broad as lateral lobes, row of eleven simple setae on distolateral margin of each medial lobe. Covered in cuticular combs.

Pleopod II (Fig. 10) protopod length 1.0 width, 0.7 pleopod I length, laterally fringed with 14 long setae submarginally and short bristles in between; endopod stylet 0.7 protopod length, slender and acute distally; exopod thickened, prominent behind distomedial margin of protopod, with tuft of fine setae.

Pleopod III (Fig. 10) opercular, 1.8 of pleopod 2 length; protopod elongate, endopod small, rounded, without any setae, exopod 1.5 as long as wide, 2.4 as long as endopod, laterally and distally fringed with short simple setae and 25 submarginal setae, distal article 1.3 as long and 1.3 as wide as proximal article.

Pleopod IV (Fig. 10) protopod length 0.7 width, endopod 1.7 exopod width and 0.7 exopod length; length 1.2 width, exopod width 0.3 length, with short setules on margins.

Distribution: Nidhogg vent and Amundsen Basin, Arctic Ocean, between 3016.5 and 4156 m depth (Fig. 4).

Habitat: Specimens of the new species from the Jøtul field were found only on precipitates collected from the Nidhogg vent (Fig. 3), a 10-m high and 30-m wide mound at water depth of 3031 m (Fig. 2). It consists of fallen hydrothermal vents and hydrothermal precipitate made up by barite, amorphous silicate and chalcophyrite traces (Bohrmann *et al.* 2024). On the mound are several smaller chimneys with water venting at 33°C (Bohrmann *et al.* 2024). The male specimen from the Amundsen Basin was found in soft sediment.

Remarks: The two species in *Bathyjaera* Kohlenbach and Linse gen. nov. look very similar. However, *B. giselae* Kohlenbach and Pereira sp. nov. can be distinguished from its congeneric species by (characters from *B. tyleri* between parentheses; Table 3): widest pereonites 3 or 4 (pereonites 6 or 7). Pleotelsonic notch, medial projection about 0.5 total notch length (0.3 total notch length). Uropodal protopod equal in length to width (protopod length 1.35 width). Maxilliped palp length 1.1 basis length (length 0.9 endite length). Antennula length longer than head (subequal in length); antenna length 0.4 body length (0.3 body length). Male pleopod I slender, medial lobes 3.5× as broad as lateral lobes (2.0× as broad). In addition, specimens of *B. giselae* Kohlenbach and Pereira sp. nov. are larger (4.2 mm) than those of *B. tyleri* (3.8 mm).

Phylogenetic results: The analyses of the *COI* sequences show that the new species described herein belongs to a different species from that of *B. tyleri* comb. nov. and other *Jaera* species (Fig. 16). The analysis of the genetic difference between both species, showed a variation of 41.6%–48.7% in the same genus and thus both *Bathyjaera* Kohlenbach and Linse gen. nov. species can be considered as two distinct species (Table 5). The uncorrected *p*-distance within *B. tyleri* comb. nov. revealed a low divergence (0%–2.8%) while it was quite broad for *B. giselae* Kohlenbach and Pereira sp. nov. with 1%–36% (Table 5). This large genetic variation in *B. giselae* Kohlenbach and Pereira sp. nov. implies that some individuals are almost as different from each other as from *B. tyleri* comb. nov.

Regarding the other taxa considered in this study, the species *Jaera istri* and *J. sarsi* were basically indistinguishable (<0.2%), as well as species belonging to the *J. albifrons* complex (<2%). However, both *Jaera* groups were distinct from *B. giselae* Kohlenbach and Pereira sp. nov. with ~30% divergence and *B. tyleri* comb. nov. with ~45% divergence (Table 5), and clearly separated from *Bathyjaera* Kohlenbach and Linse gen. nov. in the *COI* and 18S analyses (Fig. 16; Supplementary Fig. S1).

Downloaded from academic.oup.com/zoolinnean/article/208/3/zlag181/9097109 by Natural Environment Research Council user on 24 November 2026

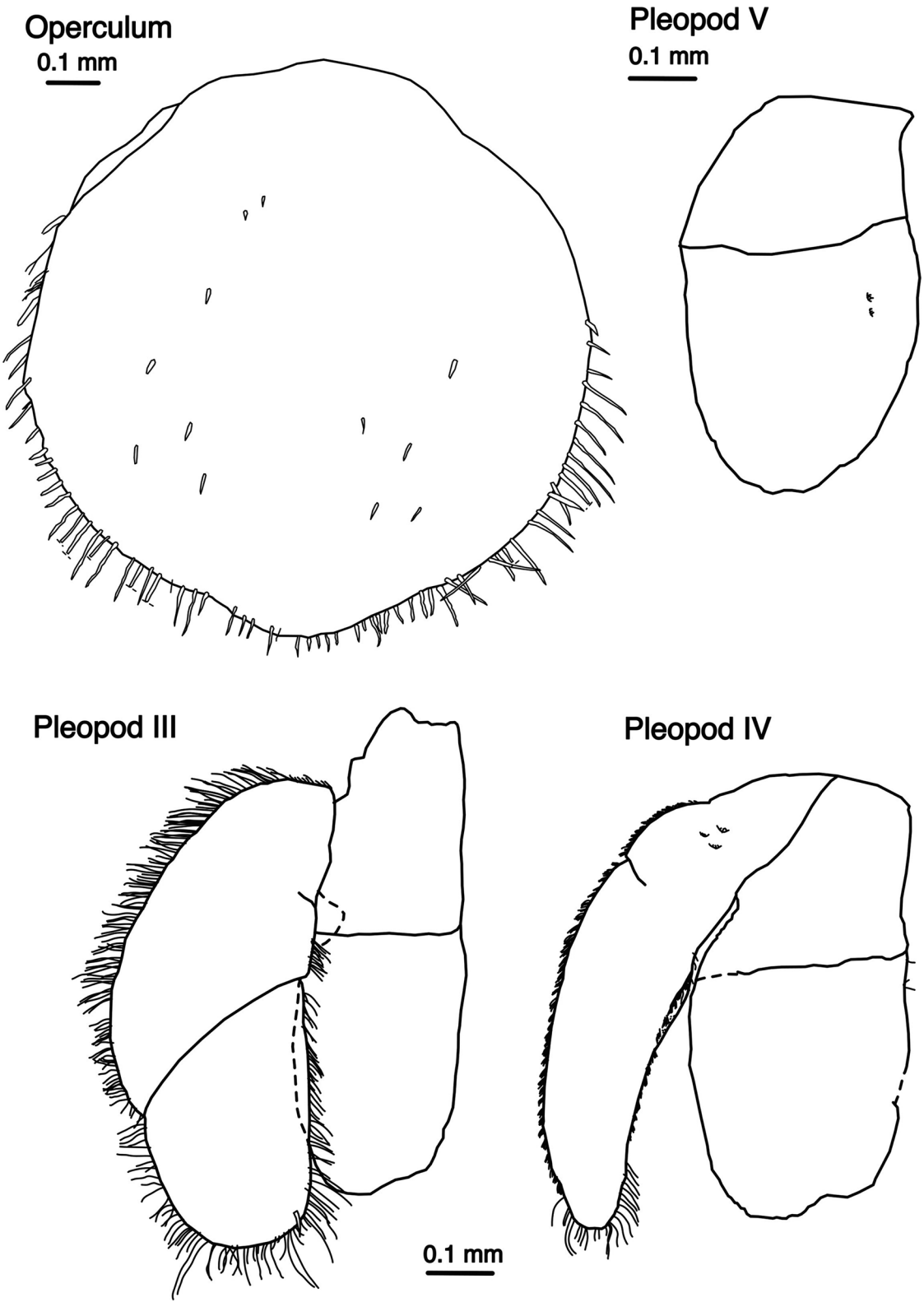

Figure 8 *Bathyjaera giselae* Kohlenbach and Pereira sp. nov. Paratype female [SMF 58538 (Senckenberg)]. Pleopods II–V. The pleopod III and pleopod IV share the same scale bar.

Downloaded from academic.oup.com/zoolinnean/article/208/3/zlag181/9097109 by Natural Environment Research Council user on 24 November 2026

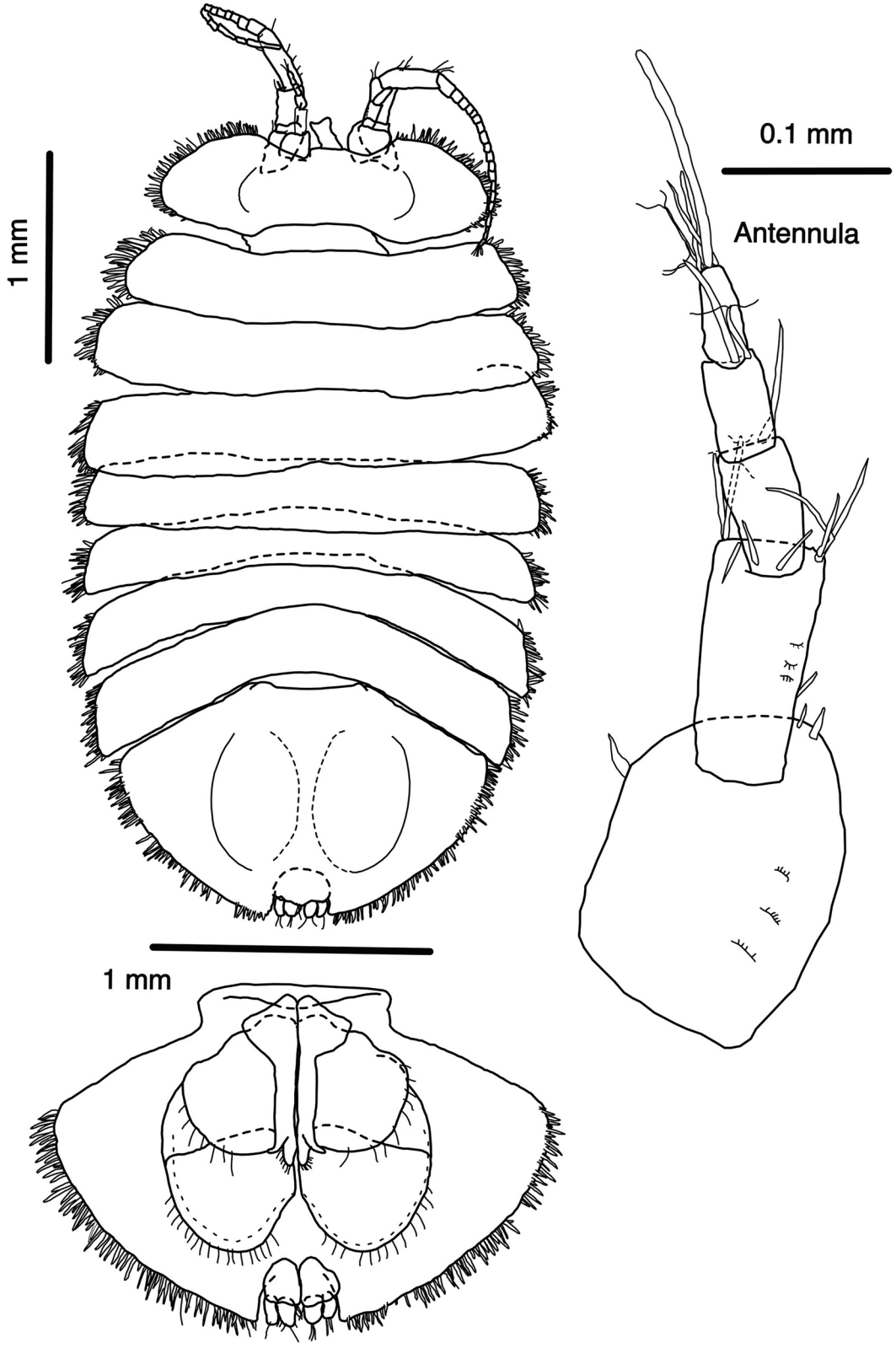

Figure 9 *Bathyjaera giselae* Kohlenbach and Pereira sp. nov. Paratype male [TSZCr-19237 (UiT)]. Habitus and antennula in dorsal view and pleotelson in ventral view.

Downloaded from academic.oup.com/zoolinnean/article/208/3/zlag181/9097109 by Natural Environment Research Council user on 24 November 2026

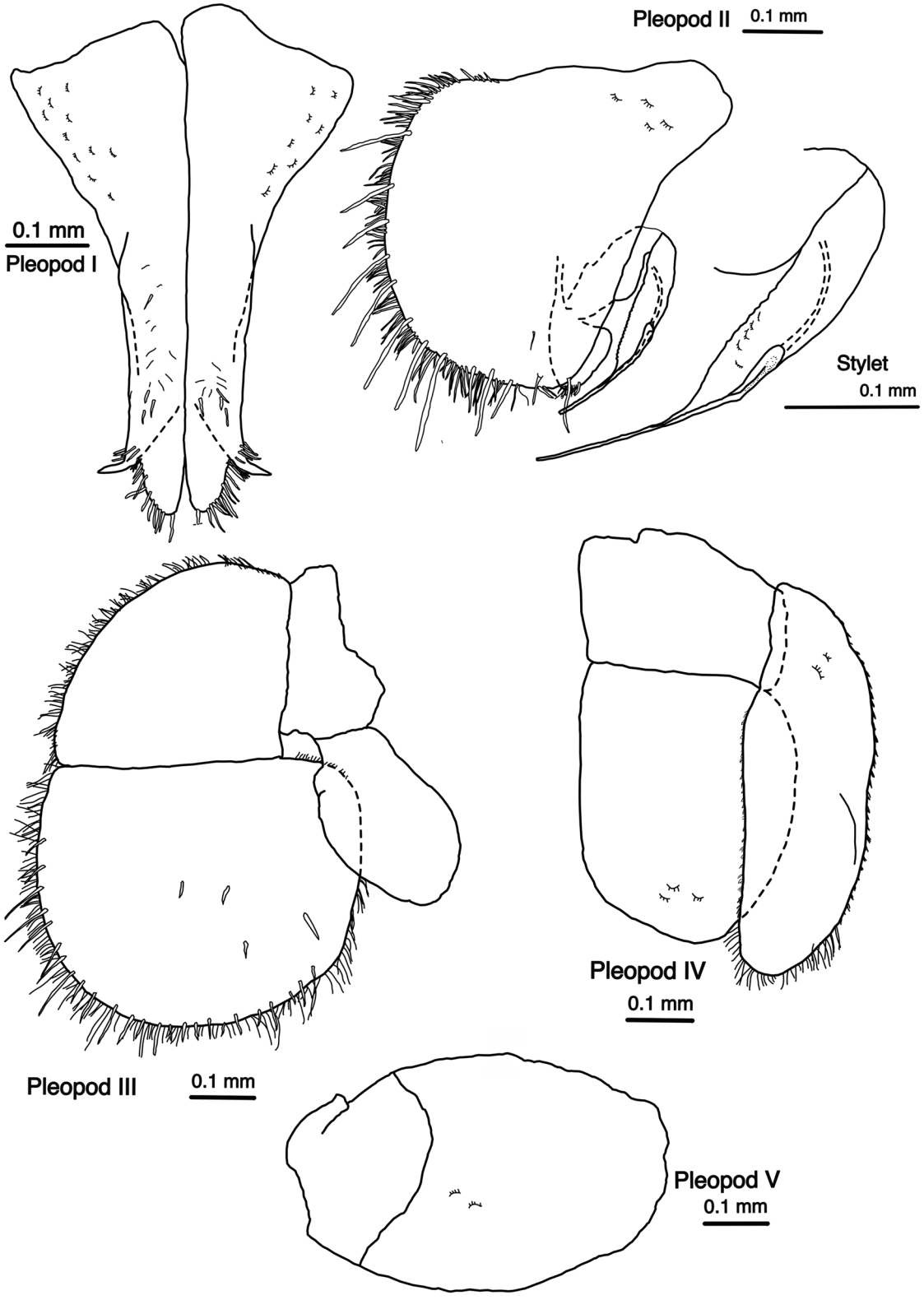

Figure 10 *Bathyjaera giselae* Kohlenbach and Pereira sp. nov. Paratype male [TSZCr-19237 (UiT)]. Pleopods I–V. Pleopod II with detail of stylet.

Downloaded from academic.oup.com/zoolinnean/article/208/3/zlag181/9097109 by Natural Environment Research Council user on 24 November 2026

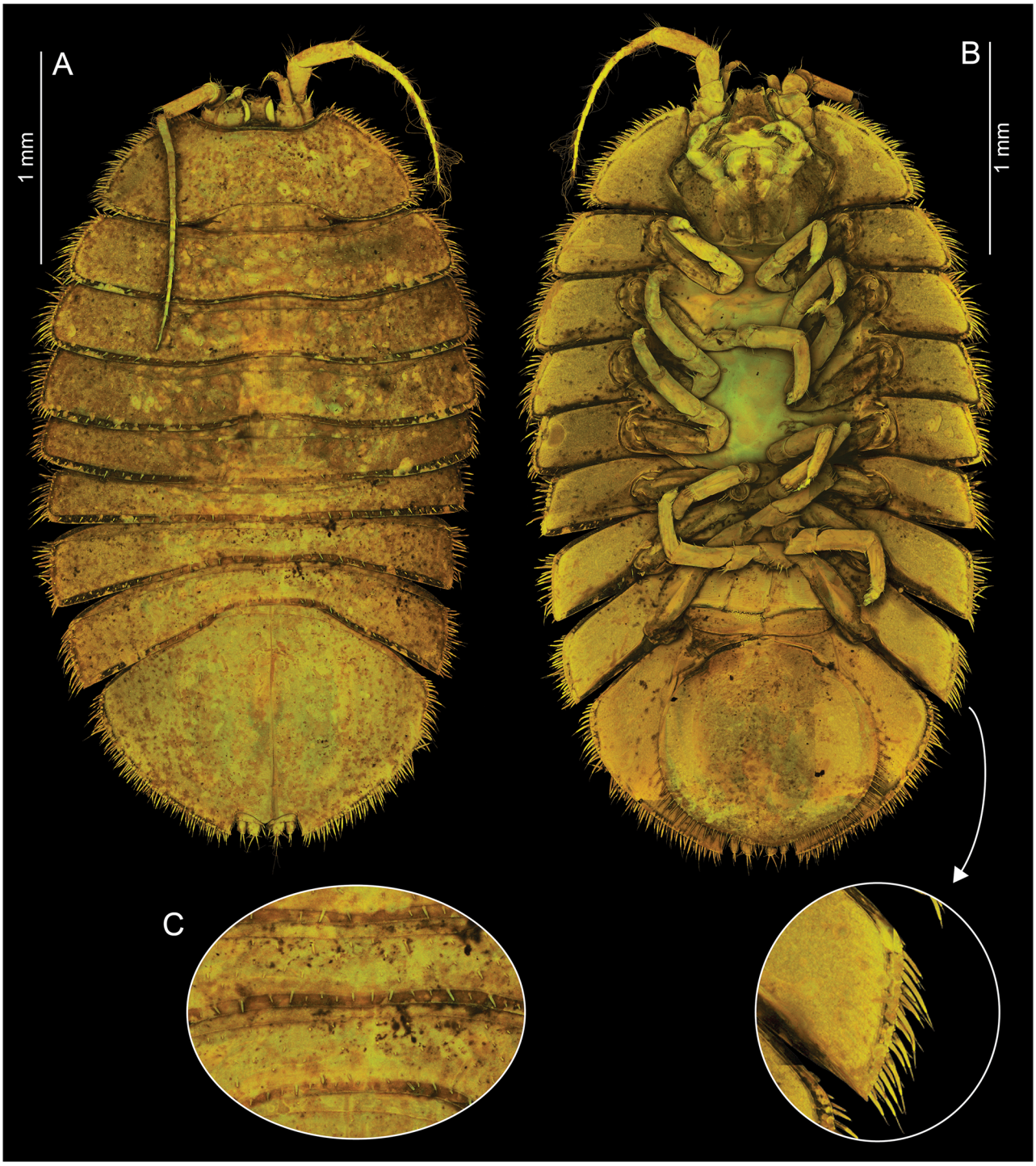

Figure 11 *Bathyjaera giselae* Kohlenbach and Pereira sp. nov. female [SMF 58539 (Senckenberg)]. CLSM photographs. Habitus in dorsal (A) and ventral (B) views, with details of spine-like setae in posterior (C) and lateral margins of pereonites. Scale = 1 mm.

Discussion

Integrative taxonomic approach

In the present contribution, the genus *Bathyjaera* Kohlenbach and Linse gen. nov. is erected to include two blind janirid species collected from chemosynthetic environments: the new species *B. giselae* Kohlenbach and Pereira sp. nov. and *B. tyleri* comb. nov. Both species show morphological characters that do not fit within the last revised diagnosis of the genus *Jaera* presented by Linse *et al.* (2014).

Although both species show similar morphological characters, the analyses of *COI* and 18S sequences (Fig. 16; Supplementary Fig. S1) confirmed that *B. tyleri* comb. nov. and *B. giselae* Kohlenbach and Pereira sp. nov. belong to two

Downloaded from academic.oup.com/zoolinnean/article/208/3/zlag181/9097109 by Natural Environment Research Council user on 24 November 2026

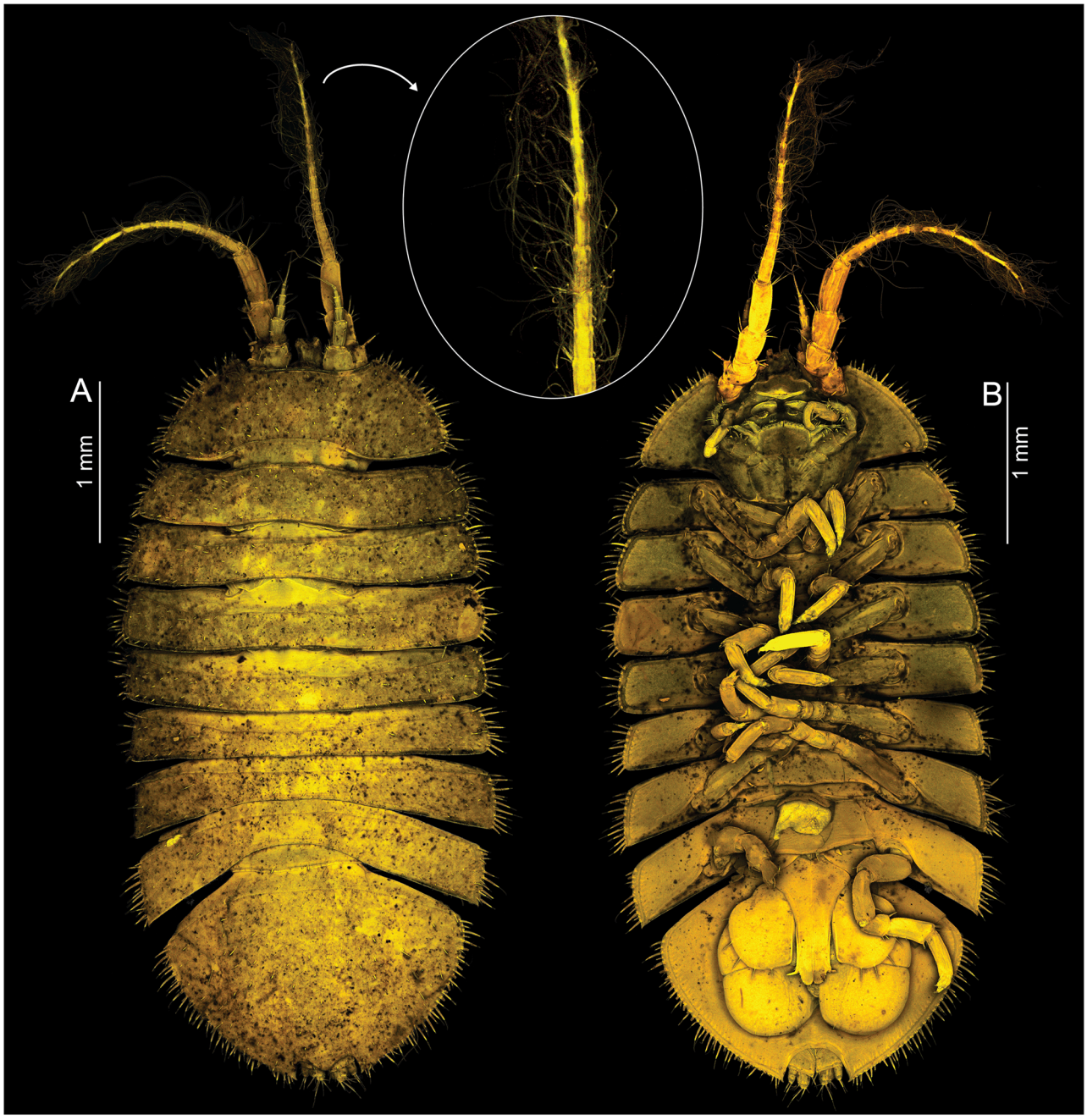

Figure 12 *Bathyjaera giselae* Kohlenbach and Pereira sp. nov. male [SMF 58540 (Senckenberg)]. CLSM photographs. Habitus in dorsal (A) and ventral (B) views, with detail of bacterial filaments visible on antenna. Scale = 1 mm.

different species. In addition, these species are differentiated from other *Jaera* species. However, the high percentage of genetic differences within the genus may suggest the presence of cryptic diversity, although additional specimens and markers are required to evaluate this hypothesis. The high divergence within *B. giselae* Kohlenbach and Pereira sp. nov. was partially due to the single specimen from the Amundsen Basin (SMF 58547), which had a strong similarity of 1% with a female from the Jøtul vent (TSZCr-19244) and a very high divergence with another female from the Jøtul vent (TSZCr-19243) of 35.7% (Table 5).

This could be due to the known issues with *COI* barcodes in the genus *Jaera* (see: Funk and Omland 2003, Nymoen *et al.* 2024) and possibly *Bathyjaera* Kohlenbach and Linse gen. nov. Depending on the studied asellote group, intraspecific divergence can be quite low or high. In the deep-sea genus *Haploniscus* Richardson, 1908, the uncorrected *p*-distance has been reported at 1.8% within species, 9%–20% between species, and 25%–28% between genera (Brix *et al.* 2011). In the family Macrostylidae Hansen, 1916, the uncorrected *p*-distance within a species could be as low as 0.1% and up to 8%, and 4.6%–37% between species (Riehl *et al.* 2018). Thus, it is difficult to compare genetic distances even within the suborder Asellota.

While the newly erected *Bathyjaera* Kohlenbach and Linse gen. nov. was supported as a distinct clade in the presented

Downloaded from academic.oup.com/zoolinnean/article/208/3/zlag181/9097109 by Natural Environment Research Council user on 24 November 2026

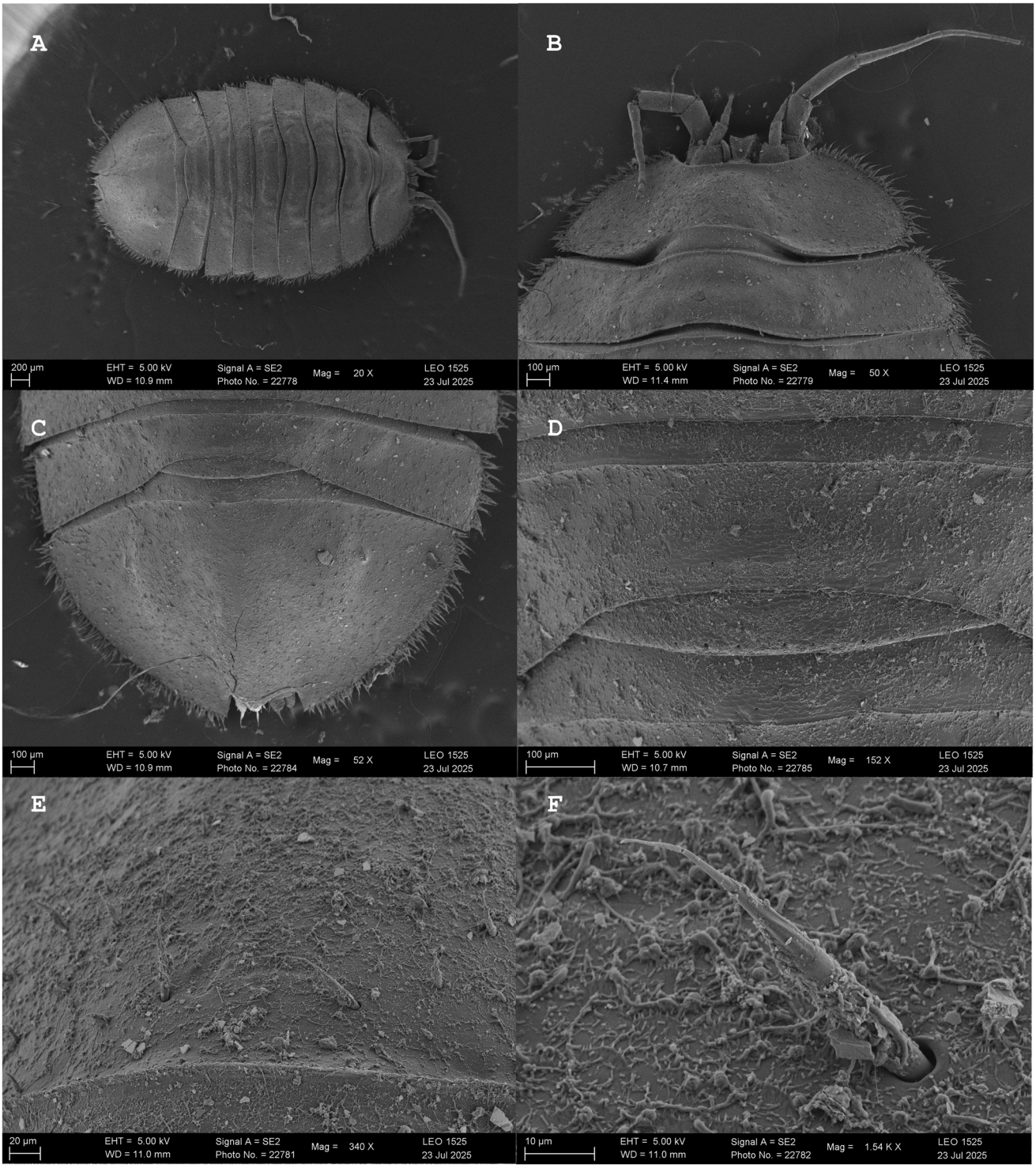

Figure 13 *Bathyjaera giselae* Kohlenbach and Pereira sp. nov. female [TSZCr-19239 (UiT)]. SEM photographs. Habitus in dorsal view (A), with details of the head (B), pleotelson (C), pleonite (D), dorsal surface (E), and a dorsal spine (F).

18S tree (Supplementary Fig. S1), it was sitting within the genus *Jaera* based on *COI*, indicating a non-monophyly of this genus (Fig. 16).

In conclusion, further investigation, including more specimens and loci, is needed to resolve generic boundaries, and the erection of the new genus *Bathyjaera* Kohlenbach and Linse gen. nov. supports the need to revise the family Janiridae. Moreover, DNA barcodes from Arctic deep-sea fauna are very scarce (Ramirez-Llodra *et al.* 2024), thus, these new *COI* and 18S barcodes are an important addition for future (meta-) barcoding studies.

Deep-sea colonization

Janirid isopods typically occur in shallow waters. In particular, the species of the genus *Jaera* have been reported from

Downloaded from academic.oup.com/zoolinnean/article/208/3/zlag181/9097109 by Natural Environment Research Council user on 24 November 2026

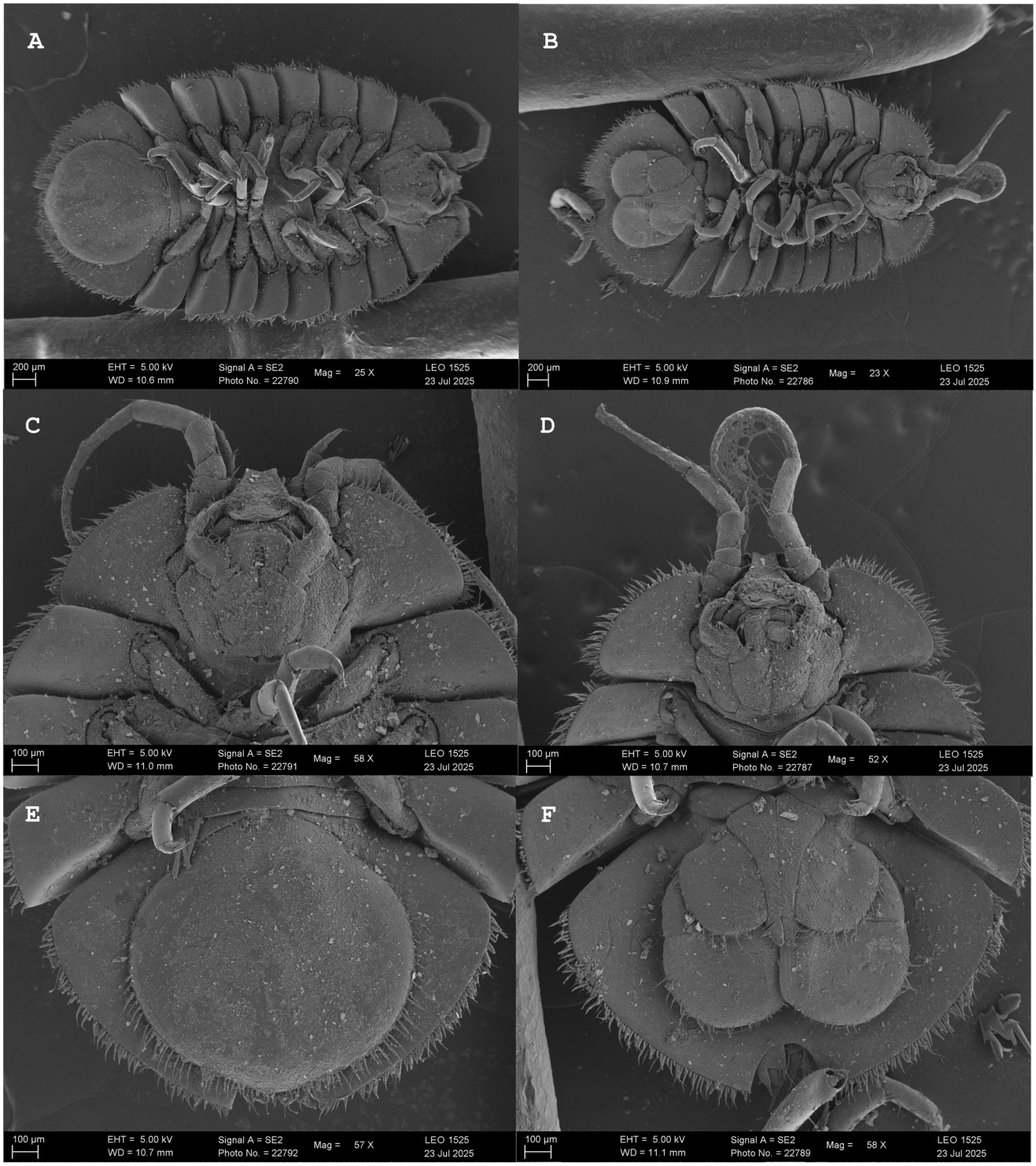

Figure 14 *Bathyjaera giselae* Kohlenbach and Pereira sp. nov. female [A, C, E, TSZCr-19240 (UiT)] and male [B, D, F, TSZCr-19241 (UiT)]. SEM photographs. Habitus in dorsal view (A + B), with details of the head (C + D), and pleotelson (E + F).

freshwater, intertidal waters, and continental shelf depth in the northern hemisphere, including the North Atlantic and Mediterranean Sea (Kesselyák 1938, Wilson and Wägele 1994, Linse *et al.* 2014), and all of them present well-developed eyes. On the other hand, the two known species of *Bathyjaera* Kohlenbach and Linse gen. nov. have been reported in the deep sea at 1144–4156 m depth, and both are blind. The presence or absence of eyes in a particular taxon can be used to infer its migration activity to or from the deep sea. The shallower bathymetric distribution of the family Janiridae and the presence of eyes on all its members suggest this family colonized the deep-sea secondarily. A similar conclusion has been reached for other isopod taxa (Brandt 1999, Raupach *et al.* 2009, Pereira and Doti 2017).

Downloaded from academic.oup.com/zoolinnean/article/208/3/zlag181/9097109 by Natural Environment Research Council user on 24 November 2026

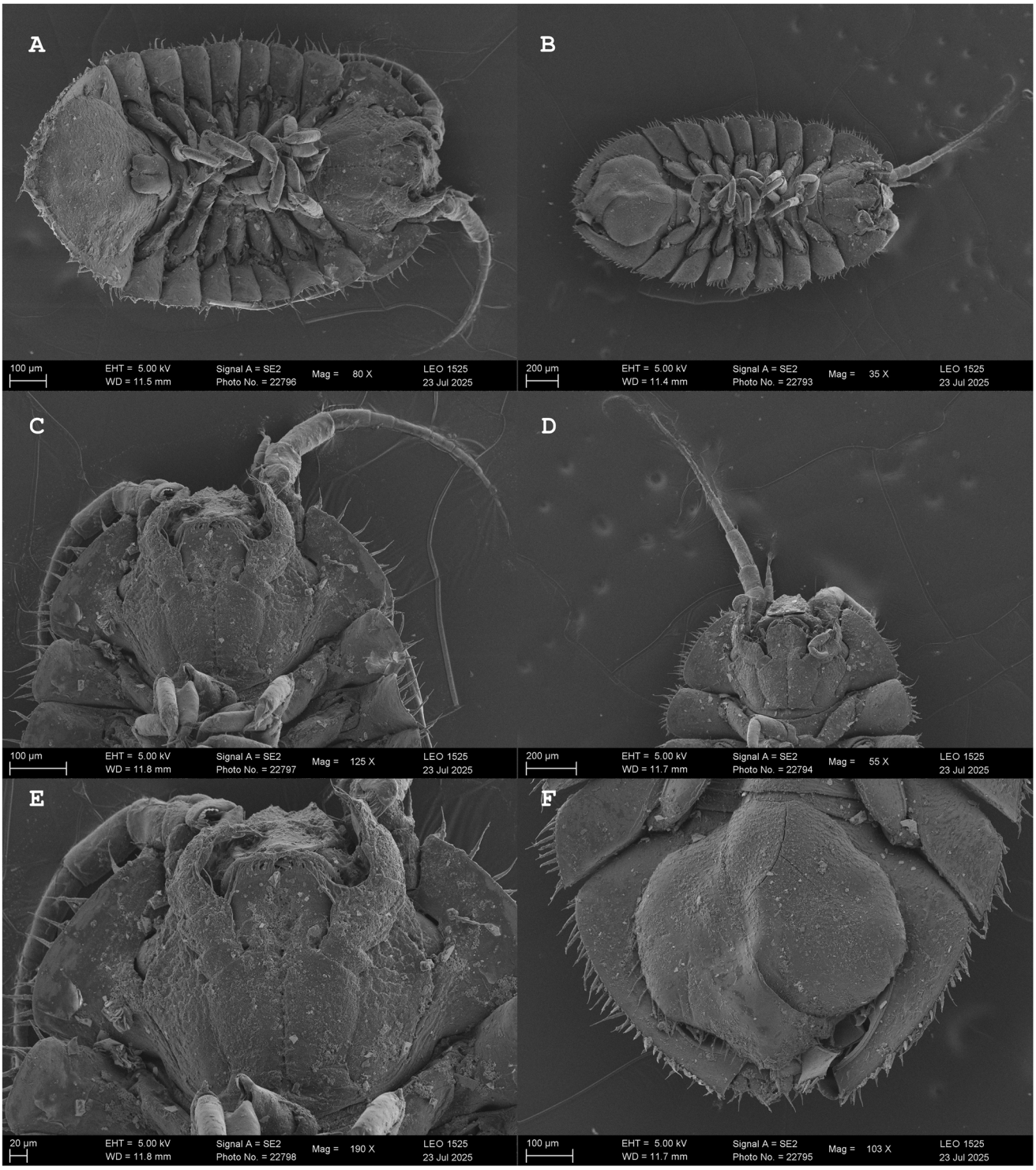

Figure 15 *Bathyjaera giselae* Kohlenbach and Pereira sp. nov. juvenile male [A, C, E, SMF 58541 (Senckenberg)] and female [B, D, F, SMF 58541 (Senckenberg)]. SEM photographs. Habitus in dorsal view (A + B), with details of the head (C + D), and pleotelson (E + F).

Distribution and feeding ecology of *Bathyjaera* gen. nov

Species of *Jaera* have been suspected of scraping off bacteria and algae from rocks and fucus since they have muscular maxillules and strongly chitinized and serrated teeth on their outer endite (Jones 1972). In the deep sea, *Bathyjaera* Kohlenbach and Linse gen. nov. inhabits chemosynthetic environments: *B. tyleri* comb. nov. was found on a whale fall in the SO (Linse *et al.* 2014) and *B. giselae* Kohlenbach and Pereira sp. nov. on an active vent field in the AO. Both species presumably feed on bacteria: *B. tyleri* comb. nov. by grazing on bacteria from the bones, and *B. giselae* Kohlenbach and Pereira sp. nov. by grazing bacteria growing on the vent. This grazing of bacterial mats can be observed generally in crustaceans on kelp and

Downloaded from academic.oup.com/zoolinnean/article/208/3/zlag181/9097109 by Natural Environment Research Council user on 24 November 2026

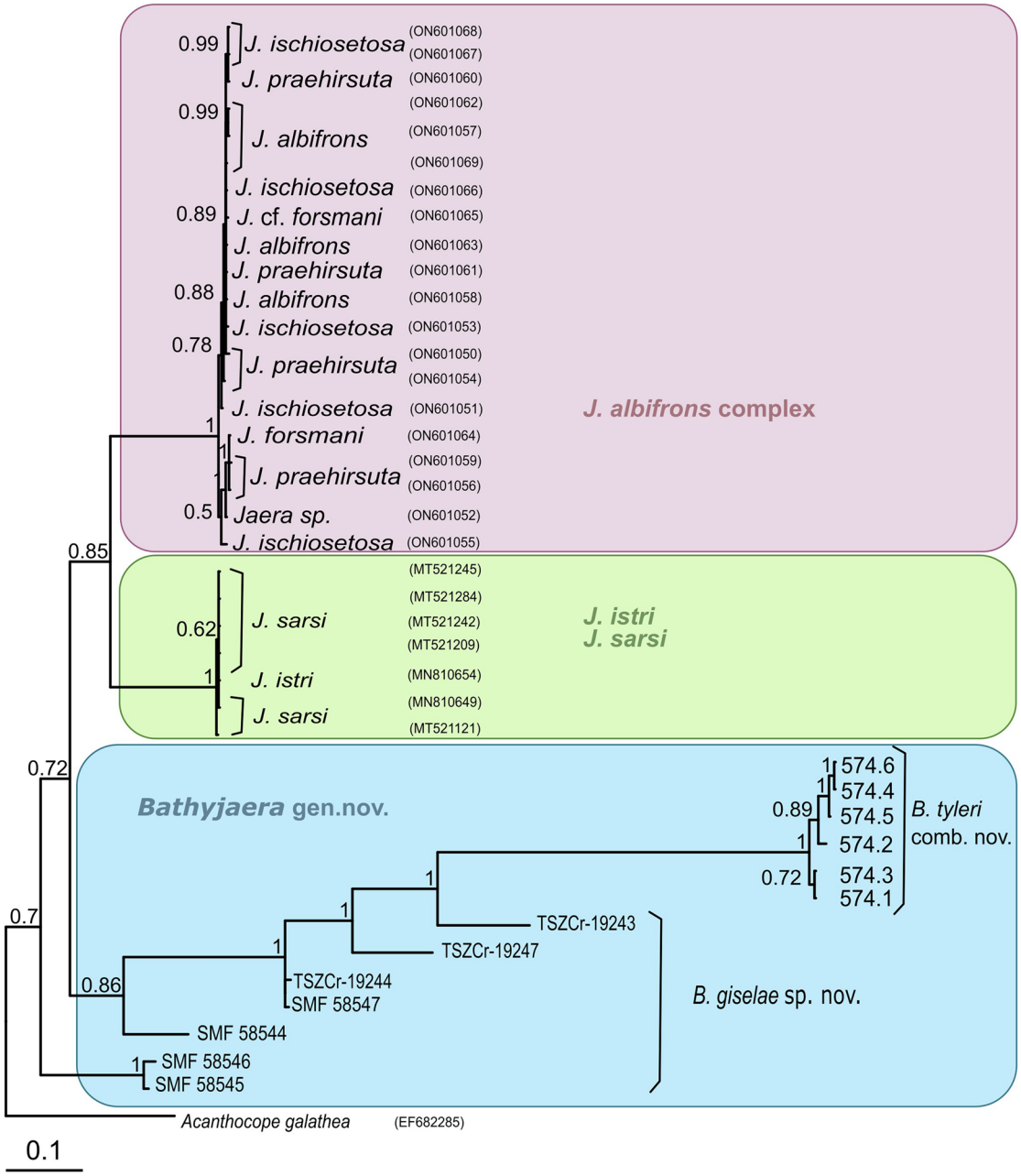

Figure 16 50% majority-rule Bayesian analysis tree using the *COI* sequences. Numbers over the branch indicate the posterior probability (PP), with PP > 0.95 considered as high support. Branches with PP lower than 0.5 are collapsed into polytomies. The tree scale bar indicates the estimated number of substitutions per site. Terminals 574.1–574.6 are *B. tyleri* comb. nov. Sequences starting with ON are species belonging to the *J. albifrons* species complex. Sequences starting with MT or MN belong to species of *J. sarsi* and *J. istri*, respectively. The outgroup is the munnopsid isopod *Acanthocope galatheae*.

wood falls (Bernardino *et al.* 2010) and in the gastropod genus *Cocculina* Dall, 1882, where *C. enigmadonta* Chen and Linse, 2020, has been found on active hydrothermal vents as well and on the same whale fall as *B. tyleri* comb. nov. in the SO (Chen and Linse 2020).

Hessler and Strömberg (1989) studied in detail the feeding mechanism of several asellote families. Among them, the authors observed that the janirid species *Janiralata occidentalis* (Walker, 1898) uses the mandibular palp to clean and scrape its antennae, and then feed on the retained fouling. As visible in the CLSM pictures (Figs 11 and 12) bacterial filaments are present on the antenna of *B. giselae* Kohlenbach and Pereira sp. nov., probably acting as an additional food source. This has also been reported from the newly described species *Eurycope andreyi* Malyutina and Golovan, 2022 from a hydrothermal vent in the Bering Sea (Malyutina and Golovan 2022).

One specimen of *B. giselae* Kohlenbach and Pereira sp. nov. (SMF 58547) was found in the Amundsen Basin in the central AO far away from (known) hydrothermal vents or other chemosynthetic environments. The other isopods found at

Downloaded from academic.oup.com/zoolinnean/article/208/3/zlag181/9097109 by Natural Environment Research Council user on 24 November 2026

Table 5 Minimum and maximum raw *COI* uncorrected *p*-distances (as %) within and between species of *Bathyjaera* Kohlenbach and Linse gen. nov. and *Jaera*.

	***B. tyleri* comb. nov.**		***B. giselae* sp. nov.**		***J. istri/J. sarsi***		***J. albifrons* complex**	
	Min	**Max**	**Min**	**Max**	**Min**	**Max**	**Min**	**Max**
B. tyleri comb. nov.	0.0	2.8						
B. giselae sp. nov.	41.6	48.7	0.1	36.0				
J. istri/J. sarsi	43.1	48.7	24.2	35.1	0.0	0.2		
J. albifrons complex	42.5	44.9	24.2	31.5	24.0	24.8	0.0	1.7

that station were typical Arctic deep-sea species and nothing indicated a chemosynthetic environment there. It might be that this specimen was transported by the inflow of Atlantic water by holding on to moving animals or kelp pieces with its pereopodal claws. At least one species of *Jaera*, *J. hopeana* Costa, 1853, has been recorded holding on to fish and using it for transport (Verhoeff 1943). No other specimen of *B. giselae* Kohlenbach and Pereira sp. nov. has been found or reported from samples in the central AO so far. *B. giselae* Kohlenbach and Pereira sp. nov. could present a patchy geographic distribution mediated by 'stepping stones' (Smith *et al.* 1989) and cover a larger habitat than expected from a vent species. Other invertebrate taxa associated with hydrothermal vents have also been found on seeps (Kiel 2016, Van Dover *et al.* 2002), wood falls (Tandberg *et al.* 2013, Chen and Linse 2020), whale falls (Bennett *et al.* 1994, Pereira *et al.* 2020b), and other decaying fauna such as mussel (De Faoite 2020). These environments can serve as stepping stones for dispersal (Smith *et al.* 1989, 2015, Van Dover *et al.* 2002, Vrijenhoek 2010).

Isopod species at hydrothermal vents

Species of isopods at hydrothermal vents are rare and often not reported at species-level (e.g. Van Dover *et al.* 1996, Wolff 2005, Taylor *et al.* 2021). Probably more isopod species live at hydrothermal vents but are difficult to sample with a remotely operating vehicle (ROV) due to their small size and quick movement. Few species have been described exclusively from hydrothermal vents (Bourdon 1983, Cunha 2006, Kato *et al.* 2022). Only recently, the first asellote isopod species were found and described in vent fields in the Bering Sea at depths of 373–472 m (Malyutina and Golovan 2022). In the present study, *B. giselae* Kohlenbach and Pereira sp. nov. is reported from the Nidhogg vent field at 1445–3156 m depth in the AO. Thus, this is the deepest record of an isopod from a hydrothermal vent field.

During the ROV dive at the Jøtul vent field, *Saduria megalura* (G.O.Sars, 1879) and *Munna acanthifera* Hansen, 1916 were sampled near the Nidhogg vent (K.K., personal observation). These are not obligate vent species but rather omnipresent in the AO (Just 1980, Svavarsson 1988) and probably benefit from the additional food input at chemosynthetic environments.

Arctic vent fauna has been hypothesized to consist of different species compared to other vents since the AO has a limited deep-sea connection to the Atlantic Ocean via the Fram Strait and due to its evolutionary history, but further sampling is needed to prove this hypothesis (Ramirez-Llodra *et al.* 2007, 2024). Dramatic changes throughout geological timescales, including full glaciation of the AO, led to mass extinctions and subsequent re-colonization via the North Atlantic and North Pacific gateways, which are mostly on continental shelves (Dunton 1992, Clarke and Crame 2010). Thus, the Arctic deep sea and its chemosynthetic habitats might harbour fewer endemic species. However, recent studies suggest deep-sea refugia, specifically at chemosynthetic habitats, in the Arctic during glacial maxima for shallow-water species (Panieri *et al.* 2025). Through that process, *Bathyjaera* Kohlenbach and Linse gen. nov. might have separated from *Jaera* and colonized the deep sea.

Conclusion

Bathyjaera Kohlenbach and Linse gen. nov. is erected based on distinct morphological and molecular differences between *B. giselae* Kohlenbach and Pereira sp. nov. and *B. tyleri* comb. nov. in comparison to species of *Jaera.* The new genus marks a first step in resolving the known polyphyly of Janiridae. The description of *B. giselae* Kohlenbach and Pereira sp. nov. adds to our limited but growing knowledge of isopods from chemosynthetic environments and their ecology, particularly in under-sampled areas, such as deep hydrothermal vents from the Arctic Ocean.

Acknowledgements

The authors acknowledge The Nippon Foundation-Nekton Ocean Census Programme (https://oceancensus.org/) for supporting the discovery and description of this species. In cooperation with REV Ocean UiT and The Arctic University of Norway, the Ocean Census supported the expedition 'Ocean Census Arctic Deep/EXTREME24' and funded the taxonomy OCAD workshop in Tromsø to where K.K. and K.L. were invited. This is Ocean Census Species Number 215. We thank the expedition leaders from the Deep Arctic–EXTREME24 on RV *Kronprins Haakon* Prof. Alex Rogers (Ocean Census) and Prof. Giuliana Panieri (University of Tromsø) and from ArcWatch-1 Prof. Antje Boetius (MBARI/AWI) and Dr Christina Bienhold (AWI), as well as the captain, crew, and scientists of RV *Kronprins Haakon*, RV *Polarstern*, Ocean Census, UiT and The Arctic University of Norway for their great work at sea and on shore. The Deep Arctic–EXTREME24 expedition received permission from NOD, The Norwegian Offshore Directorate, to collect data from the Jøtul vent site. This is publication number

Downloaded from academic.oup.com/zoolinnean/article/208/3/zlag181/9097109 by Natural Environment Research Council user on 24 November 2026

99 that uses data from the Senckenberg am Meer Confocal Laserscanning Microscope Facility (SGN-SaM-cLSM). We particularly thank Nicole Gatzemeier (DZMB) for her help in the genetic laboratory, Zhehao Hu (DZMB/Universität Hamburg) for his help assembling the sequences, calculating the genetic trees, and revising the molecular method section, Terue Cristina Kihara (INES) for her introduction into the CLSM, and Elke Wölken (Universität Hamburg) for her help with the SEM images. Kathrin Philipps-Bussau (LIB-Hamburg Museum) assisted with the loan of type material at the Zoological Museum Hamburg. Karen Jeskulke, Sven Hoffmann and Antje Fischer are thanked for sample management via the DZMB database. We are grateful for the map created by Yvonne Schulze Tenberge (AWI), and we appreciate the support of Oliver Mulville (Ocean Census), who provided the video frame grabs of the Nidhogg vent taken with ROV *Aurora*. This publication (#006–25) includes molecular data partly generated with the support of the LIB–Center for Molecular Biodiversity Research's Molecular Laboratory in Hamburg.

Author contributions

Katharina Kohlenbach (conceptualization, methodology, formal analysis, writing—original draft, visualization); Emanuel Pereira (methodology, writing—review and editing, visualization); Saskia Brix (methodology, resources, writing—review and editing, supervision); and Katrin Linse (conceptualization, resources, writing—review and editing, visualization, supervision)

Supplementary material

Supplementary material is available at *Zoological Journal of the Linnean Society* online.

Conflicts of interest

The authors declare no competing interests.

Funding

We are grateful for the ALONGate project funded via the Leibniz Programme for Woman Professors (P150/2023) to S.B. K.K. is thankful for the funding through the Hector Fellow Academy. E.P. is particularly indebted to the German Academy Exchange Service (DAAD) for the Short-Term grant received in 2024 (ID 57698958).

Data availability

All genetic data are stored in the Barcode of Life Database (BoLD) project BAJAE, which contains all available data and is publicly available. Specimens are stored in the Museum of the University of Tromsø and Senckenberg Research Institute and Natural History Museum Frankfurt.

Ethical approval

No approval of research ethics committees was required to accomplish the goals of this study because experimental work was conducted with an unregulated invertebrate species. Sampling and field studies: All necessary permits for sampling have been obtained by the authors from the competent authorities.

References

Altekar G, Dwarkadas S, Huelsenbeck JP *et al.* Parallel metropolis coupled Markov chain Monte Carlo for Bayesian phylogenetic inference. *Bioinformatics* 2004;**20**:407–15. https://doi.org/10.1093/bioinformatics/btg427

Astrin JJ, Stüben PE. Phylogeny in cryptic weevils: molecules, morphology and new genera of western Palaearctic Cryptorhynchinae (Coleoptera: Curculionidae). *Invertebrate Systematics* 2008;**22**:503–22. https://doi.org/10.1071/IS07057

Beaulieu SE, Szafrański KM. InterRidge global database of active submarine hydrothermal vent fields v.3.4, [dataset] *PANGAEA*, 2020. https://doi.org/10.1594/PANGAEA.917894

Bennett BA, Smith CR, Glaser B *et al.* Faunal community structure of a chemoautotrophic assemblage on whale bones in the deep northeast Pacific Ocean. *Marine Ecology Progress Series* 1994;**108**:205–23.

Bernardino AF, Smith CR, Baco A *et al.* Macrofaunal succession in sediments around kelp and wood falls in the deep NE Pacific and community overlap with other reducing habitats. *Deep Sea Research Part I: Oceanographic Research Papers* 2010;**57**:708–23. https://doi.org/10.1016/j.dsr.2010.03.004

Bluhm BA, Kosobokova KN, Carmack EC. A tale of two basins: an integrated physical and biological perspective of the deep Arctic Ocean. *Progress in Oceanography* 2015;**139**:89–121. https://doi.org/10.1016/j.pocean.2015.07.011

Bober S, Brix S, Riehl T *et al.* Does the Mid-Atlantic Ridge affect the distribution of abyssal benthic crustaceans across the Atlantic Ocean? *Deep Sea Research Part II: Topical Studies in Oceanography* 2018;**148**:91–104. https://doi.org/10.1016/j.dsr2.2018.02.007

Boetius A, Bienhold C. *The Expedition PS138 of the Research Vessel Polarstern to the Arctic Ocean in 2023*. Bremerhaven: Alfred-Wegener-Institute for Polar- and Marine Research, 2024. https://doi.org/10.57738/BzPM_0788_2024

Bohrmann G, Streuff K, Romer M *et al.* Discovery of the first hydrothermal field along the 500-km-long Knipovich Ridge offshore Svalbard (the Jøtul field). *Scientific Reports* 2024;**14**:10168. https://doi.org/10.1038/s41598-024-60802-3

Bourdon R. Thermaloniscus cotylophorus n. g., n. sp., premier Isopode Epicaride recolte récolté dans une zone hydrothermale oceéanique. *Revue Suisse De Zoologie* 1983;**90**:907–11. https://doi.org/10.5962/bhl.part.82015

Brandt A. On the origin and evolution of Antarctic Peracarida (Crustacea, Malacostraca). *Scientia Marina* 1999;**63**:261–74. https://doi.org/10.3989/scimar.1999.63s1261

Brandt A. SO293 AleutBio (Aleutian Trench Biodiversity Studies) Cruise Report/Fahrtbericht, Cruise No. SO293, 24.07.2022 - 06.09.2022, Dutch Harbor (USA)—Vancouver (Canada), Sonne Berichte 2022. https://doi.org/10.48433/cr_so293

Brandt A, Brenke N, Andres HG *et al.* Diversity of peracarid crustaceans (Malacostraca) from the abyssal plain of the Angola Basin. *Organisms Diversity and Evolution* 2005;**5**:105–12. https://doi.org/10.1016/j.ode.2004.10.007

Downloaded from academic.oup.com/zoolinnean/article/208/3/zlag181/9097109 by Natural Environment Research Council user on 24 November 2026

Brandt A, Brix S, Brökeland W *et al.* Deep-sea isopod biodiversity, abundance, and endemism in the Atlantic sector of the Southern Ocean—results from the ANDEEP I–III expeditions. *Deep Sea Research Part II: Topical Studies in Oceanography* 2007a;**54**:1760–75. https://doi.org/10.1016/j.dsr2.2007.07.015

Brandt A, De Broyer C, De Mesel I *et al.* The biodiversity of the deep Southern Ocean benthos. *Philosophical Transactions of the Royal Society of London. Series B, Biological Sciences* 2007b;**362**:39–66. https://doi.org/10.1098/rstb.2006.1952

Brandt A, Gooday AJ, Brandao SN *et al.* First insights into the biodiversity and biogeography of the Southern Ocean deep sea. *Nature* 2007c;**447**:307–11. https://doi.org/10.1038/nature05827

Brandt A, Alalykina I, Fukumori H *et al.* First insights into macrofaunal composition from the SokhoBio expedition (Sea of Okhotsk, Bussol Strait and northern slope of the Kuril-Kamchatka Trench). *Deep Sea Research Part II: Topical Studies in Oceanography* 2018;**154**:106–20. https://doi.org/10.1016/j.dsr2.2018.05.022

Brenke N. An epibenthic sledge for operations on marine soft bottom and bedrock. *Marine Technology Society Journal* 2005;**39**:10–21. https://doi.org/10.4031/002533205787444015

Brix S, Riehl T, Leese F. First genetic data for species of the genus *Haploniscus* Richardson, 1908 (Isopoda: Asellota: Haploniscidae) from neighbouring deep-sea basins in the South Atlantic. *Zootaxa* 2011;**2838**:79–84. https://doi.org/10.11646/zootaxa.2838.1.5

Brix S, Svavarsson J, Leese F. A multi-gene analysis reveals multiple highly divergent lineages of the isopod *Chelator insignis* (Hansen, 1916) south of Iceland. *Polish Polar Research* 2014;**35**:225–42. https://doi.org/10.2478/popore-2014-0015

Brix S, Leese F, Riehl T *et al.* A new genus and new species of Desmosomatidae Sars, 1897 (Isopoda) from the eastern South Atlantic abyss described by means of integrative taxonomy. *Marine Biodiversity* 2015;**45**:7–61. https://doi.org/10.1007/s12526-014-0218-3

Brix S, Stransky B, Malyutina M *et al.* Distributional patterns of isopods (Crustacea) in Icelandic and adjacent waters. *Marine Biodiversity* 2018a;**48**:783–811. https://doi.org/10.1007/s12526-018-0871-z

Brix S, Bober S, Tschesche C *et al.* Molecular species delimitation and its implications for species descriptions using desmosomatid and nannoniscid isopods from the VEMA fracture zone as example taxa. *Deep Sea Research Part II: Topical Studies in Oceanography* 2018b;**148**:180–207. https://doi.org/10.1016/j.dsr2.2018.02.004

Brix S, Osborn KJ, Kaiser S *et al.* Adult life strategy affects distribution patterns in abyssal isopods–implications for conservation in Pacific nodule areas. *Biogeosciences* 2020;**17**:6163–84. https://doi.org/10.5194/bg-17-6163-2020

Chen C, Linse K. From wood to vent: first cocculinid limpet associated with hydrothermal activity discovered in the Weddell Sea. *Antarctic Science* 2020;**32**:354–66. https://doi.org/10.1017/S095410202000022X

Clarke A, Crame JA. Evolutionary dynamics at high latitudes: speciation and extinction in polar marine faunas. *Philosophical Transactions of the Royal Society of London. Series B, Biological Sciences* 2010;**365**:3655–66. https://doi.org/10.1098/rstb.2010.0270

Cunha MR. Arthropoda, Crustacea, Isopoda. In: Desbruyères D, Segonzac M, Bright M (eds), *Handbook of Deep-sea Hydrothermal Vent Fauna. Denisia*. Linz, Austria: Biologiezentrum der Oberösterreichischen Landesmuseen, 2006:18.

De Faoite FG. Dead mussels as food-stepping stone habitats for deep-sea hydrothermal fauna, [Master's thesis, Utrecht University], 2020. https://studenttheses.uu.nl/handle/20.500.12932/39141

Dreyer H, Wägele JW. Parasites of crustaceans (Isopoda: Bopyridae) evolved from fish parasites: molecular and morphological evidence. *Zoology* 2001;**103**:157–78.

Dunton K. Arctic biogeography: the paradox of the marine benthic fauna and flora. *Trends in Ecology and Evolution* 1992;**7**:183–9.

Folmer O, Black M, Hoeh W *et al.* DNA primers for amplification of mitochondrial cytochrome c oxidase subunit I from diverse metazoan invertebrates. *Molecular Marine Biology and Biotechnology* 1994;**3**:294–9.

Funk DJ, Omland KE. Species-level paraphyly and polyphyly: frequency, causes, and consequences, with insights from animal mitochondrial DNA. *Annual Review of Ecology, Evolution, and Systematics* 2003;**34**:397–423. https://doi.org/10.1146/annurev.ecolsys.34.011802.132421

GEBCO Bathymetric Compilation Group. The GEBCO_2024 Grid—a continuous terrain model of the global oceans and land, 2024. https://doi.org/10.5285/1C44CE99-0A0D-5F4F-E063-7086ABC0EA0F

GLIMS Consortium. (2005), *GLIMS Glacier Database, Version 1*. Boulder, Colorado USA: NASA National Snow and Ice Data Center Distributed Active Archive Center. https://doi.org/https://doi.org/10.7265/N5V98602

Hendriks L, Goris A, Neefs JM *et al.* The nucleotide sequence of the small ribosomal subunit RNA of the yeast *Candida albicans* and the evolutionary position of the fungi among the eukaryotes. *Systematic and Applied Microbiology* 1989;**12**:223–9. https://doi.org/10.1016/S0723-2020(89)80066-9

Hessler RR. The Desmosomatidae (Isopoda, Asellota) of the Gay Head–Bermuda transect. *Bulletin of the Scripps Institution of Oceanography* 1970;**15**:1–185.

Hessler RR, Strömberg J. Behavior of janiroidean isopods (Asellota), with special reference to deep-sea genera. *Sarsia* 1989;**74**:145–59. https://doi.org/10.1080/00364827.1989.10413424

Hessler RR, Thistle D. On the place of origin of deep-sea Isopods. *Marine Biology* 1975;**32**:155–65. https://doi.org/10.1007/BF00388508

Hessler RR, Wilson GD, Thistle D. The deep-sea isopods: a biogeographic and phylogenetic overview. *Sarsia* 1979;**64**:67–75. https://doi.org/10.1080/00364827.1979.10411365

Howat I. *MEaSUREs Greenland Ice Mapping Project (GIMP) Land Ice and Ocean Classification Mask. (NSIDC-0714, Version 1)*. Boulder, Colorado, USA: NASA National Snow and Ice Data

Downloaded from academic.oup.com/zoolinnean/article/208/3/zlag181/9097109 by Natural Environment Research Council user on 24 November 2026

Center Distributed Active Archive Center, 2017. https://doi.org/10.5067/B8X58MQBFUPAIHO-IOCGEBCO, www.gebco.net

Jakobsson M, Mayer LA, Bringensparr C *et al.* The international bathymetric chart of the Arctic Ocean v.4.0. *Scientific Data* 2020;**7**:176. https://doi.org/10.1038/s41597-020-0520-9

Jones MB. The mouthparts of the members of the *Jaera albifrons* group of species (Crustacea: Isopoda). *Marine Biology* 1972;**14**:264–70. https://doi.org/10.1007/BF00348290

Just J. Abyssal and deep bathyal Malacostraca (Crustacea) from the Polar Sea. *Videnskabelige Meddelelser Fra Dansk Naturhistorisk Forening* 1980;**142**:161–77.

Kaiser S, Barnes DKA, Linse K *et al.* Epibenthic macrofauna associated with the shelf and slope of a young and isolated Southern Ocean island. *Antarctic Science* 2008;**20**:281–90. https://doi.org/10.1017/s0954102008001107

Kato N, Chen C, Watanabe HK *et al.* The first bopyrid isopod from hydrothermal vents: *Pleurocryptella shinkai* sp. nov. (Isopoda: Epicaridea) parasitizing *Shinkaia crosnieri* (Decapoda: Anomura). *Zoological Science* 2022;**39**:293. https://doi.org/10.2108/zs210117

Katoh K, Rozewicki J, Yamada KD. MAFFT online service: multiple sequence alignment, interactive sequence choice and visualization. *Briefings in Bioinformatics* 2019;**20**:1160–6. https://doi.org/10.1093/bib/bbx108

Kearse M, Moir R, Wilson A *et al.* Geneious basic: an integrated and extendable desktop software platform for the organization and analysis of sequence data. *Bioinformatics* 2012;**28**:1647–9. https://doi.org/10.1093/bioinformatics/bts199

Kesselyák A. Die Arten der Gattung *Jaera* Leach (Isopoda, Asellota). *Zoologischer Jahrbücher für Systematik* 1938;**71**:21952.

Kiel S. A biogeographic network reveals evolutionary links between deep-sea hydrothermal vent and methane seep faunas. *Proceedings of the Royal Society B: Biological Sciences* 2016;**283**:20162337. https://doi.org/10.1098/rspb.2016.2337

Kihara TC, da Rocha CEF. *Técnicas Para Estudos Taxonômico de Copépodes Harpacticóides da Meiofauna Marinha*. Porto Alegre: Asterisco, 2009.

Knauber H, Silberberg JR, Brandt A *et al.* Evolution and biogeography of the *Haploniscus belyaevi* species complex (Isopoda: Haploniscidae) revealed by means of integrative taxonomy. *Systematics and Biodiversity* 2022;**20**:1–27. https://doi.org/10.1080/14772000.2022.2099477

Kohlbach D, Fransson A, Amargant-Arumi M *et al.* Nansen and Amundsen basins: gradients of physico-chemical properties and biota composition with implications for future resource management of the central Arctic Ocean. *Elementa: Science of the Anthropocene* 2025;**13**:00016. https://doi.org/10.1525/elementa.2024.00016

Kürzel K, Brix S, Brandt A *et al.* Pan-Atlantic comparison of deep-sea macro-and megabenthos. *Diversity* 2023;**15**:814. https://doi.org/10.3390/d15070814

Kumar S, Stecher G, Suleski M *et al.* Molecular Evolutionary Genetics Analysis v.12 for adaptive and green computing. *Molecular Biology and Evolution* 2024;**41**:1–9. https://doi.org/10.1093/molbev/msae263

Linse K, Jackson JA, Malyutina MV *et al.* Shallow-water northern hemisphere *Jaera* (Crustacea, Isopoda, Janiridae) found on whale bones in the southern ocean deep sea: ecology and description of *Jaera tyleri sp. nov. PLoS One* 2014;**9**:e93018. https://doi.org/10.1371/journal.pone.0093018

Macheriotou L, Rossel S, Molari M *et al.* Connectivity in the Clarion–Clipperton Zone: a review. *Frontiers in Marine Science* 2025;**12**:1547803. https://doi.org/10.3389/fmars.2025.1547803

Malyutina MV, Brandt A. Munnopsidae (Crustacea, Isopoda, Asellota) from the Kuril–Kamchatka Trench with a regional and inter-ocean comparison of their biogeographic and richness patterns. *Progress in Oceanography* 2020;**183**:102289. https://doi.org/10.1016/j.pocean.2020.102289

Malyutina MV, Golovan OA. The first record of Asellota (Isopoda) from hydrothermal vent biotopes of the submarine Piip Volcano, Bering Sea, with descriptions of two new species of Munnopsidae. *Deep Sea Research Part II: Topical Studies in Oceanography* 2022;**202**:105137. https://doi.org/10.1016/j.dsr2.2022.105137

Michels J, Büntzow M. Assessment of Congo red as a fluorescence marker for the exoskeleton of small crustaceans and the cuticle of polychaetes. *Journal of Microscopy* 2010;**238**:95–101. https://doi.org/10.1111/j.1365-2818.2009.03360.x

Minh BQ, Schmidt HA, Chernomor O *et al.* IQ-TREE 2: new models and efficient methods for phylogenetic inference in the genomic era. *Molecular Biology and Evolution* 2020;**37**:1530–1534. https://doi.org/10.1093/molbev/msaa015

Nymoen AR, Kongsrud JA, Willassen E *et al.* When standard DNA barcodes do not work for species identification: intermixed mitochondrial haplotypes in the *Jaera albifrons* complex (Crustacea: Isopoda). *Marine Biodiversity* 2024;**54**:43. https://doi.org/10.1007/s12526-024-01435-7

Panieri G, Argentino C, Savini A *et al.* Sanctuary for vulnerable Arctic species at the Borealis Mud Volcano. *Nature Communications* 2025;**16**:504. https://doi.org/10.1038/s41467-024-55712-x

Paradis E, Schliep K. Ape 5.0: an environment for modern phylogenetics and evolutionary analyses in R. *Bioinformatics* 2019;**35**:526–528. https://doi.org/10.1093/bioinformatics/bty633

Pereira E, Doti BL. *Edotia abyssalis* n. sp. from the Southwest Atlantic Ocean, first record of the genus (Isopoda, Valvifera, Idoteidae) in the deep sea. *Zoologischer Anzeiger* 2017;**268**:19–31. https://doi.org/10.1016/j.jcz.2017.04.007

Pereira E, Roccatagliata D, Doti BL. Xiphoarcturus-a new genus and two new species of the family Antarcturidae (Isopoda: Valvifera) from the Mar del Plata submarine canyon and its phylogenetic relationships. *Arthropod Systematics and Phylogeny* 2019;**77**:303–23. https://doi.org/10.26049/ASP77-2-2019-07

Pereira E, Roccatagliata D, Doti BL. On the antarcturid genus *Fissarcturus* (Isopoda: Valvifera): description of *Fissarcturus argentinensis* n. sp., first description of the male of *Fissarcturus patagonicus* (Ohlin, 1901), and biogeographic remarks

Downloaded from academic.oup.com/zoolinnean/article/208/3/zlag181/9097109 by Natural Environment Research Council user on 24 November 2026

on the genus. *Zoologischer Anzeiger* 2020a;**288**:168–189. https://doi.org/10.1016/j.jcz.2020.08.002

Pereira OS, Shimabukuro M, Bernardino AF *et al.* Molecular affinity of southwest Atlantic *Alvinocaris muricola* with Atlantic equatorial belt populations. *Deep Sea Research Part I: Oceanographic Research Papers* 2020b;**163**:103343. https://doi.org/10.1016/j.dsr.2020.103343

Pereira E, Doti BL, Roccatagliata D. A new species of *Pseudione sensu lato* (Isopoda: Bopyridae) on a squat lobster host from the deep South-West Atlantic. *Zootaxa* 2021;**4996**:363–373. https://doi.org/10.11646/zootaxa.4996.2.10

Pereira E, Roccatagliata D, Doti BL. Revision of the genus *Oxyarcturus* (Isopoda, Valvifera, Antarcturidae), with a description of a new deep-sea species from Argentina. *Zoosystematics and Evolution* 2023;**99**:457–72. https://doi.org/10.3897/zse.99.106667

Pereira E, Roccatagliata D, Corriale MJ *et al.* Into the deep: diversity of valviferan isopods (Crustacea: Peracarida) from the Mar del Plata submarine canyon and adjacent area, Argentina. *Deep Sea Research Part I: Oceanographic Research Papers* 2025;**222**:104515. https://doi.org/10.1016/j.dsr.2025.104515

Posit Team. *RStudio: Integrated Development Environment for R.* PBC, Boston, MA: Posit Software, 2025.

Ramirez-Llodra E, Shank TM, German CR. Biodiversity and biogeography of hydrothermal vent species–thirty years of discovery and investigation. *Oceanography* 2007;**20**:30–41. https://doi.org/10.5670/oceanog.2007.78

Ramirez-Llodra E, Meyer HK, Bluhm BA *et al.* The emerging picture of a diverse deep Arctic Ocean seafloor: from habitats to ecosystems. *Elementa: Science of the Anthropocene* 2024;**12**:00140. https://doi.org/10.1525/elementa.2023.00140

Rambaut A, Drummond AJ, Xie D *et al.* Posterior summarization in Bayesian phylogenetics using Tracer 1.7. *Systematic Biology* 2018;**67**:901–904. https://doi.org/10.1093/sysbio/syy032

Raupach MJ, Mayer C, Malyutina M *et al.* Multiple origins of deep-sea Asellota (Crustacea: Isopoda) from shallow waters revealed by molecular data. *Proceedings of the Royal Society B: Biological Sciences* 2009;**276**:799–808. https://doi.org/10.1098/rspb.2008.1063

R Development Core Team. *R: A language and environment for statistical computing*. Vienna, Austria: R Foundation for Statistical Computing, 2021.

Riehl T, Brandt A. Descriptions of two new species in the genus *Macrostylis* Sars, 1864 (Isopoda Asellota Macrostylidae) from the Weddell Sea (Southern Ocean), with a synonymisation of the genus *Desmostylis* Brandt, 1992 with *Macrostylis*. *ZooKeys* 2010;**57**:9–49. https://doi.org/10.3897/zookeys.57.310

Riehl T, Lins L, Brandt A. The effects of depth, distance, and the Mid-Atlantic Ridge on genetic differentiation of abyssal and hadal isopods (Macrostylidae). *Deep Sea Research Part II: Topical Studies in Oceanography* 2018;**148**:74–90. https://doi.org/10.1016/j.dsr2.2017.10.005

Rogers AD, Panieri G, Angeles IB *et al.* Ocean Census Arctic Deep Expedition report (Leg 1, EXTREME24) [report]. Oxford: Nippon Foundation–Nekton Ocean Census; 2024:1–197. https://oceancensus.org/expeditions/arctic-deep/

Ronquist F, Teslenko M, van der Mark P *et al.* MrBayes 3.2: efficient Bayesian phylogenetic inference and model choice across a large model space. *Systematic Biology* 2012;**61**:539–542. https://doi.org/10.1093/sysbio/sys029

Schnurr S, Osborn KJ, Malyutina M *et al.* Hidden diversity in two species complexes of munnopsid isopods (Crustacea) at the transition between the northernmost North Atlantic and the Nordic Seas. *Marine Biodiversity* 2018;**48**:813–843. https://doi.org/10.1007/s12526-018-0877-6

Schwarz G. Estimating the dimension of a model. *The Annals of Statistics* 1978;**6**:461–464.

Smith CR, Kukert H, Wheatcroft RA *et al.* Vent fauna on whale remains. *Nature* 1989;**341**:27–28. https://doi.org/10.1038/341027a0

Smith CR, Glover AG, Treude T *et al.* Whale-fall ecosystems: recent insights into ecology, paleoecology, and evolution. *Annual Review of Marine Science* 2015;**7**:571–96. https://doi.org/10.1146/annurev-marine-010213-135144

Stecher G, Tamura K, Kumar S. Molecular evolutionary genetics analysis (MEGA) for macOS. *Molecular Biology and Evolution* 2020;**37**:1237–1239. https://doi.org/10.1093/molbev/msz312

Svavarsson J. Bathyal and abyssal Asellota (Crustacea, Isopoda) from the Norwegian, Greenland, and North Polar Seas). *Sarsia* 1988;**73**:83–106. https://doi.org/10.1080/00364827.1988.10420676

Tandberg AH, Rapp HT, Schander C *et al.* Exitomelita sigynae gen. et sp. nov.: a new amphipod from the Arctic Loki Castle vent field with potential gill ectosymbionts. *Polar Biology* 2012;**35**:705–16. https://doi.org/10.1007/s00300-011-1115-x

Tandberg AHS, Rapp HT, Schander C *et al.* A new species of Exitomelita (Amphipoda: Melitidae) from a deep-water wood fall in the northern Norwegian Sea. *Journal of Natural History* 2013;**47**:1875–89. https://doi.org/10.1080/00222933.2012.725778

Tandberg AHS, Vader W, Olsen BR *et al. Monoculodes bousfieldi* sp. n. from the Arctic hydrothermal vent Loki's Castle. *Marine Biodiversity* 2018;**48**:927–37. https://doi.org/10.1007/s12526-018-0869-6

Taylor J, Devey CW, Le Saout M *et al.* The discovery and preliminary geological and faunal descriptions of three new Steinahóll vent sites, Reykjanes Ridge, Iceland. *Frontiers in Marine Science* 2021;**8**:520713. https://doi.org/10.3389/fmars.2021.520713

Van Dover CL, Desbruyères D, Segonzac M *et al.* Biology of the Lucky Strike hydrothermal field. *Deep Sea Research Part I: Oceanographic Research Papers* 1996;**43**:1509–29. https://doi.org/10.1016/S0967-0637(96)00051-9

Van Dover CL, German CR, Speer KG *et al.* Evolution and biogeography of deep-sea vent and seep invertebrates. *Science (New York, N.Y.)* 2002;**295**:1253–7. https://doi.org/10.1126/science.1067361

Verhoeff KW. Zur Morphologie, Ökologie und Systematik von *Sphaeroma, Europosphaera* und *Jaera* (85.

Downloaded from academic.oup.com/zoolinnean/article/208/3/zlag181/9097109 by Natural Environment Research Council user on 24 November 2026

Isopoden-Aufsatz). *Zeitschrift für Morphologie und Ökologie der Tiere* 1943;**40**:276–90.

Vrijenhoek RC. Genetic diversity and connectivity of deep-sea hydrothermal vent metapopulations. *Molecular Ecology* 2010;**19**:4391–411. https://doi.org/10.1111/j.1365-294X.2010.04789.x

Wang L-G, Lam TT-Y, Xu S *et al.* treeio: an R package for phylogenetic tree input and output with richly annotated and associated data. *Molecular Biology and Evolution* 2020;**37**:599–603. https://doi.org/10.1093/molbev/msz240

Wickham H, Averick M, Bryan J *et al.* Welcome to the tidyverse. *Journal of Open Source Software* 2019;**4**:1686. https://doi.org/10.21105/joss.01686

Wilmotte A, Van der Auwera G, De Wachter R. Structure of the 16S ribosomal RNA of the thermophilic cyanobacterium *Chlorogloeopsis* HTF (‘*Mastigocladus laminosus*’HTF) strain PCC7518, and phylogenetic analysis. *FEBS Letters* 1993;**317**:96–100. https://doi.org/10.1016/0014-5793(93)81499-P

Wilson G. A systematic revision of the deep-sea subfamily Lipomerinae of the isopod crustacean family Munnopsidae. *Bulletin of the Scripps Institution of Oceanography* 1989;**27**:1–138.

Wilson GDF. A phylogenetic analysis of the isopod family Janiridae (Crustacea). *Invertebrate Taxonomy* 1994;**8**:749–66. https://doi.org/10.1071/IT9940749

Wilson GDF. A new family of Asellota (Crustacea, Isopoda) from the deep sea of Zealandia. *European Journal of Taxonomy* 2024;**917**:122–51. https://doi.org/10.5852/ejt.2024.917.2393

Wilson GDF, Wägele JW. Review of the family Janiridae (Crustacea: Isopoda: Asellota). *Invertebrate Taxonomy* 1994;**8**:683–747. https://doi.org/10.1071/IT9940683

Wolff T. The systematics and biology of bathyal and abyssal Isopoda Asellota. *Galathea Report* 1962;**6**:1–320.

Wolff T. Composition and endemism of the deep-sea hydrothermal vent fauna. *CBM-Cahiers de Biologie Marine* 2005;**46**:97–104.

Yu G, Smith D, Zhu H *et al.* ggtree: an R package for visualization and annotation of phylogenetic trees with their covariates and other associated data. *Methods in Ecology and Evolution* 2017;**8**:28–36. https://doi.org/10.1111/2041-210X.12628

Downloaded from academic.oup.com/zoolinnean/article/208/3/zlag181/9097109 by Natural Environment Research Council user on 24 November 2026

© The Author(s) 2026. Published by Oxford University Press on behalf of The Linnean Society of London.
This is an Open Access article distributed under the terms of the Creative Commons Attribution License (https://creativecommons.org/licenses/by/4.0/), which permits unrestricted reuse, distribution, and reproduction in any medium, provided the original work is properly cited. Zoological Journal of the Linnean Society 2026 208(3) 1–30
https://doi.org/10.1093/zoolinnean/zlag181
Original Article